

A MONTE CARLO SIMULATION OF X-RAY FLUORESCENCE TO
DETERMINE THE INTER-ELEMENT EFFECTS IN
X-RAY SPECTROCHEMICAL ANALYSIS

by

Fernando Luis Benitez-Garcia

A Dissertation Submitted to the Faculty of the
DEPARTMENT OF METALLURGICAL ENGINEERING

In Partial Fulfillment of the Requirements
For the Degree of

DOCTOR OF PHILOSOPHY
WITH A MAJOR IN METALLURGY

In the Graduate College

THE UNIVERSITY OF ARIZONA

1 9 7 7

INFORMATION TO USERS

This material was produced from a microfilm copy of the original document. While the most advanced technological means to photograph and reproduce this document have been used, the quality is heavily dependent upon the quality of the original submitted.

The following explanation of techniques is provided to help you understand markings or patterns which may appear on this reproduction.

1. The sign or "target" for pages apparently lacking from the document photographed is "Missing Page(s)". If it was possible to obtain the missing page(s) or section, they are spliced into the film along with adjacent pages. This may have necessitated cutting thru an image and duplicating adjacent pages to insure you complete continuity.
2. When an image on the film is obliterated with a large round black mark, it is an indication that the photographer suspected that the copy may have moved during exposure and thus cause a blurred image. You will find a good image of the page in the adjacent frame.
3. When a map, drawing or chart, etc., was part of the material being photographed the photographer followed a definite method in "sectioning" the material. It is customary to begin photoing at the upper left hand corner of a large sheet and to continue photoing from left to right in equal sections with a small overlap. If necessary, sectioning is continued again — beginning below the first row and continuing on until complete.
4. The majority of users indicate that the textual content is of greatest value, however, a somewhat higher quality reproduction could be made from "photographs" if essential to the understanding of the dissertation. Silver prints of "photographs" may be ordered at additional charge by writing the Order Department, giving the catalog number, title, author and specific pages you wish reproduced.
5. PLEASE NOTE: Some pages may have indistinct print. Filmed as received.

Xerox University Microfilms

300 North Zeeb Road
Ann Arbor, Michigan 48106

77-26,966

BENITEZ-GARCIA, Fernando Luis, 1938-
A MONTE CARLO SIMULATION OF X-RAY FLUORESCENCE TO DETERMINE THE INTER-ELEMENT EFFECTS IN X-RAY SPECTROCHEMICAL ANALYSIS.

The University of Arizona, Ph.D.,
1977
Engineering, metallurgy

Xerox University Microfilms, Ann Arbor, Michigan 48106

A MONTE CARLO SIMULATION OF X-RAY FLUORESCENCE TO
DETERMINE THE INTER-ELEMENT EFFECTS IN
X-RAY SPECTROCHEMICAL ANALYSIS

by

Fernando Luis Benitez-Garcia

A Dissertation Submitted to the Faculty of the
DEPARTMENT OF METALLURGICAL ENGINEERING

In Partial Fulfillment of the Requirements
For the Degree of

DOCTOR OF PHILOSOPHY
WITH A MAJOR IN METALLURGY

In the Graduate College

THE UNIVERSITY OF ARIZONA

1 9 7 7

THE UNIVERSITY OF ARIZONA

GRADUATE COLLEGE

I hereby recommend that this dissertation prepared under my direction by Fernando L. Benitez-Garcia entitled A Monte Carlo Simulation of X-Ray Fluorescence to Determine the Inter-element Effects in X-Ray Spectrochemical Analysis be accepted as fulfilling the dissertation requirement for the degree of Doctor of Philosophy

H. Alan Jine
Dissertation Director

July 4, 1977
Date

As members of the Final Examination Committee, we certify that we have read this dissertation and agree that it may be presented for final defense.

Milind V. Chaudal

June 29, 1977

T. M. Morris

June 30, 1977

Louisa J. Demer

June 30, 1977

Daniel J. Muepfler

June 29, 1977

Gordon H. Seiger

June 27, 1977

Final approval and acceptance of this dissertation is contingent on the candidate's adequate performance and defense thereof at the final oral examination.

STATEMENT BY AUTHOR

This dissertation has been submitted in partial fulfillment of requirements for an advanced degree at The University of Arizona and is deposited in the University Library to be made available to borrowers under rules of the Library.

Brief quotations from this dissertation are allowable without special permission, provided that accurate acknowledgment of source is made. Requests for permission for extended quotation from or reproduction of this manuscript in whole or in part may be granted by the head of the major department or the Dean of the Graduate College when in his judgment the proposed use of the material is in the interests of scholarship. In all other instances, however, permission must be obtained from the author.

SIGNED: Fernando Benitez Garcia

ACKNOWLEDGMENTS

The author wishes to express his gratitude to Professor H. Alan Fine for his valuable guidance, cooperation, and constant encouragement throughout the course of this investigation.

The author also wishes to sincerely thank his wife, Sara, for her devotion, understanding, constant encouragement, and love. Her sacrifice made it possible.

Special thanks are due to the members of the Metallurgical Engineering Department for their stimulating conversations.

Financial assistance was provided by the Metallurgical Engineering Department.

TABLE OF CONTENTS

	Page
LIST OF TABLES	vi
LIST OF ILLUSTRATIONS	vii
ABSTRACT	viii
1. INTRODUCTION	1
2. LITERATURE REVIEW	3
2.1 Analytical Methods	5
2.1.1 Standard Addition and Dilution Method	7
2.1.2 Calibration Standardization Methods	8
2.1.3 Standardization with Scattered X-Rays	10
2.1.4 Dilution Methods	10
2.1.5 Thin-Film Methods	11
2.2 Mathematical Methods	12
2.2.1 The Influence Coefficient Method	12
2.2.2 The Fundamental Parameters Method	16
2.2.3 Simulation Techniques	19
3. SIMULATION TECHNIQUE	20
3.1 Derivation of the Monte Carlo Model	27
3.1.1 Random Wavelength Source	30
3.1.2 Length of the Free Path	31
3.1.3 The Colliding Atom	33
3.1.4 Sample Interactions	34
3.1.5 Secondary Emission	35
3.1.6 Scattering	36
3.1.7 Emission or Scattering Direction	36
3.1.8 Collision Coordinate	38
3.2 Description of the Flow Chart	39
3.3 The Influence Coefficients	49
3.4 Validation of the Monte Carlo Model	51
4. SIMULATION RESULTS	52

TABLE OF CONTENTS--Continued

	Page
5. DISCUSSION OF RESULTS	63
5.1 The Statistical Error	63
5.2 Energy Source	65
5.3 Inaccuracy of the X-Ray Data	68
5.4 Analytical Results	68
6. SUMMARY AND CONCLUSIONS	71
7. SUGGESTIONS FOR FUTURE WORK	72
APPENDIX A: X-RAYS, A FORTRAN IV PROGRAM FOR THE MONTE CARLO SIMULATION OF THE X-RAY FLUORESCENCE PROCESS	73
APPENDIX B: X-RAYSA, A FORTRAN IV PROGRAM FOR NUMERICAL REGRESSION ANALYSIS	82
LIST OF REFERENCES	86

LIST OF TABLES

Table		Page
4.1	X-Ray Data	53
4.2	The Effect of the Mass Absorption Coefficient on the Relative Intensity	56
4.3	The Effect of the Fluorescent Yield on the Relative Intensity	57
4.4	Predicted Relative Intensities	58
4.5	Inter-Element Coefficients for the Ternary System Ni-Cr-Fe .	60
4.6	Calculated Concentrations (Weight Fractions)	61
4.7	Calculated Relative Errors (%)	62
5.1	Effect of the Number of Photons on the Relative Intensity . .	64
5.2	Inter-Element Coefficients for the Ternary System Ni-Cr-Fe .	69

LIST OF ILLUSTRATIONS

Figure		Page
2.1	Mutual Enhancement and Absorption Effects of Elements A and B	4
2.2	Calibration Curves Illustrating the Matrix Effects on the Analyte-Line Intensity	6
3.1	Secondary Emission of Element i , Excited by the Primary X-Ray Beam, and Element j Radiation	21
3.2	Absorption through a Slab of Thickness t	23
3.3	X-Ray Fluorescence Model	28
3.4	Probability Distribution Analogy	33
3.5	Spherical Coordinates System for the Emission or Scattering Direction	37
3.6	Flow Chart for Program X-RAYS	40
4.1	Effect of the Number of Trajectories on the Predicted Relative Intensity	54
5.1	Comparison between the 45 kV CP and 45 kV FWR Random Wavelength Distribution	67

ABSTRACT

A Monte Carlo model was developed to simulate the x-ray fluorescence process within a homogeneous multi-element mixture. The model was designed to simulate the x-ray fluorescence process in conventional x-ray units, in which the sample is excited with a continuous spectrum of exciting radiation. The model was applied to an alloy system in which the inter-element effects are severe. The model was verified with experimental data on similar samples. The results indicate that the Monte Carlo model is a practical simulator for the x-ray fluorescence process, with an associated error of less than 10%, which is probably as accurately as the model parameters (particularly the fluorescent yield) are known.

CHAPTER 1

INTRODUCTION

X-ray fluorescence spectroscopy has been widely used for the compositional analysis of various materials such as metal alloys, slags, ores, refractory materials, and others. It is applicable over an extremely wide concentration range, from 100% for any element above fluorine in atomic number to 0.0001% for sensitive elements in favorable matrices. The high speed and degree of precision attainable are especially attractive features of this technique.

As applied to quantitative analysis, x-ray fluorescence spectroscopy is based on the measurement of the intensity of the characteristic radiation of the analyte, or element of interest, when it is excited with x-rays. The relationship between the measured intensity and the concentration of the analyte can be expressed graphically or by means of regression analysis correlation equations based on samples of known concentrations, i.e., standards.

The three main sources of errors in x-ray fluorescence spectroscopy are: 1) the instability of the spectrometer and associated electronic equipment; 2) heterogeneity in the sample, such as particle size, surface defects, and segregation; and 3) the inter-element effects resulting from the chemical nature of the sample. Recent equipment developments and sample preparation techniques, such as dilution, chemical separation, and fusion, have contributed to reduce the first two

sources of errors to an insignificant level. Therefore, the main concern of the x-ray spectroscopist is to correct for the matrix effects of the associated elements on the analyte-line intensity.

Several methods have been developed to eliminate or minimize the inter-element effects. The use of standards has provided the means to establish calibration curves and correction factors. The addition of dilutants and absorbers to the sample reduces the interactions of the individual elements to such an extent that the resulting calibration curves are straight lines. However, sample contamination, limited applications, and time consumption are some of the disadvantages and/or restrictions of these methods. Many empirical and theoretical methods have also been applied for the correlation of the analyte-line intensity and concentration.

The present work is aimed at studying the inter-element or matrix effects on the analyte-line intensity by the associated elements present in a homogeneous multi-element mixture. This was achieved by a Monte Carlo simulation of the x-ray fluorescence process, in which photons with random energy are forced to interact within a sample of known composition. The path histories of the photons as they move through the sample are recorded and all the events involved in the fluorescence process are analyzed to determine the degree of interference or matrix effects. The influence coefficients thus determined were, in turn, used in a regression equation to determine the analyte's concentrations from measured intensity data.

CHAPTER 2

LITERATURE REVIEW

The effect of total sample composition on the fluorescent intensity of the analyte lines has been studied by many investigators, as will be discussed in the following sections. In addition to the change of intensity of the analyte line with its concentration, variations occur with changes in concentration of the other elements in the sample. The effects of the associated elements on the analyte-line intensity are designated synonymously as matrix, inter-element, and absorption-enhancement effects. The matrix effects may arise from the following phenomena: 1) the matrix absorbs the primary radiation that could excite the analyte line; 2) the matrix absorbs the analyte radiation; and 3) one or more of the elements present in the sample emit characteristic or secondary radiation that could excite the analyte to emit additional characteristic lines (Bertin, 1970).

If the $K\alpha_A$ line of element A occurs at a wavelength just less than the absorption-edge wavelength of element B (Fig. 2.1), where the absorption-edge wavelength, λ_{abs} , is the wavelength corresponding to the minimum energy required to excite a given characteristic line in an atom, the $K\alpha_A$ radiation is absorbed by element B. Furthermore, if the $K\alpha_B$ line is, in turn, excited by element A, then the $K\alpha_B$ line intensity is enhanced in proportion to A and the $K\alpha_A$ is reduced in proportion to B. The relationship between the A- and B-line intensity and its concentration

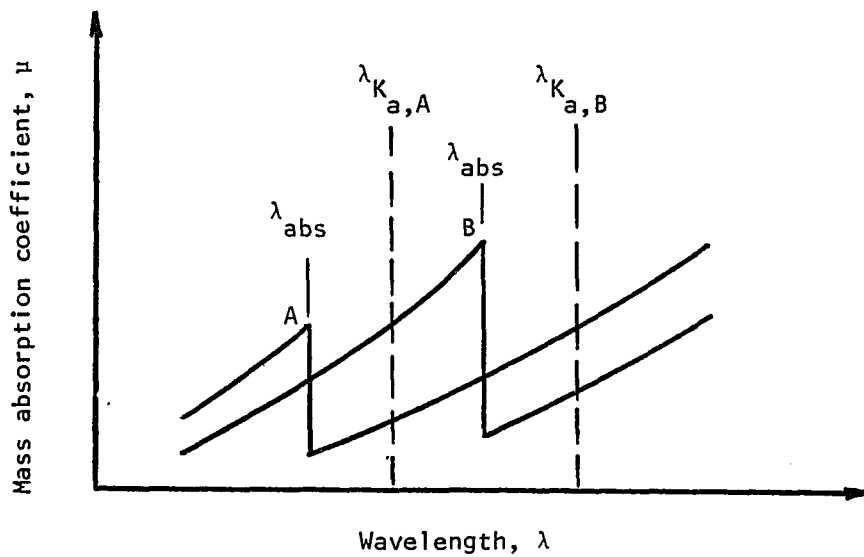


Fig. 2.1 Mutual Enhancement and Absorption Effects of Elements A and B.
-- Mass absorption coefficient vs. wavelength.

in a multi-element mixture can be illustrated graphically (Fig. 2.2). Curve A represents the ideal case, where the absorption characteristic of the matrix is substantially the same as the analyte for both the primary and analyte radiation. Absorption effect of B on A is illustrated in curve B, where element B strongly absorbs primary and A-line radiation, and the measured A-line intensity is smaller than would be expected. Enhancement of B by A is illustrated in curve C, where A lines excite the B atoms to produce additional characteristic lines, and the measured B-line intensity is larger than would be expected. Therefore, the prediction of the inter-element effects is of great importance in x-ray secondary emission spectroscopy. The matrix effects are systematic, predictable, and readily evaluated (Jenkins and de Vries, 1967). Thus, several analytical and mathematical methods have been developed to eliminate, minimize, circumvent, and/or correct for these inter-element or matrix effects.

2.1 Analytical Methods

For quantitative analysis, it is necessary to relate the measured fluorescent intensity to the concentration (weight fraction) of the analyte in the sample. As a first approximation, the spectral-line intensity of element A in a homogeneous matrix, M, is proportional to its concentration, as given by the following equation,

$$I_{A,M} = C_{A,M} I_{A,A} , \quad (2.1)$$

where $C_{A,M}$ is the weight fraction or concentration of analyte A in matrix M, and $I_{A,A}$ is the line intensity in pure A. Even under ideal

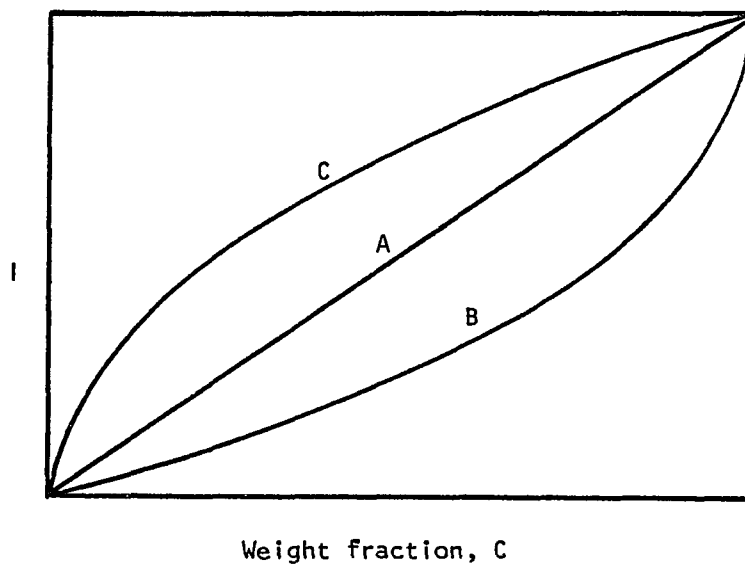


Fig. 2.2 Calibration Curves Illustrating the Matrix Effects on the Analyte-Line Intensity -- Intensity vs. weight fraction.

operational conditions, Equation (2.1) seldom applies, as the analyte intensity is also a function of the other elements in the matrix, M,

$$I_{A,M} = F_n (I_{A,A}, C_{A,M}, M) , \quad (2.2)$$

where the matrix, M, consists of the entire specimen, except the particular analyte under consideration. Thus, in a multi-element mixture, the matrix of the same specimen is different for each element present. The most widely used methods to determine the precise composition with the aid of standard samples of known composition are discussed below.

2.1.1 Standard Addition and Dilution Method

This method usually requires few standards or calibration curves, which makes it suitable to samples that are not frequently analyzed. It is only applicable to trace and minor analysis, where the analyte-line intensity vs. concentration is assumed to be linear.

Campbell and Carl (1954, 1956) treated a sample, X, with a standard material, S, containing a known concentration of the analyte, C_S , thus forming a mixture, XS, having concentration C_{XS} . Then the measured analyte-line intensities from both the untreated and treated samples were related to the original concentration as follows,

$$C_X = C_S (I_X / I_{XS}) / [1 - (I_X / I_{XS}) C_{XS}] . \quad (2.3)$$

Wagner and Bryan (1966) used a similar method, but instead treated both the sample and the standard with the same amount of an inert dilutant containing no analyte. Similar techniques or methods have also been used

by Gunn (1957), Hakkila and Waterbury (1960), Rose (1960), Lambert (1959), and other investigators.

2.1.2 Calibration Standardization Methods

Most x-ray fluorescence spectrometric analysis now in use is based on comparison of the analyte-line intensity measured from the sample with several well-analyzed standards. The standards must be similar to the samples with regard to: 1) physical form; 2) analytical composition; and 3) physical features, such as particle size, surface finish, and packing density. The analysis is done by measuring the analyte-line intensity from the sample. Then comparison of this intensity with a calibration curve or mathematical calibration factor (Müller, 1972) is made to determine the analyte concentration.

Instead of the total measured intensity, several investigators have used an intensity ratio. Andermann and Allen (1961) used the ratio of the analyte intensity to the background intensity. Jones (1961) used the intensity ratio between the analyte line and some reference element added to the sample. Cullen (1962) used the ratio of the analyte intensity to the coherently scattered target lines.

Hirokawa (1962) used a two-standard method to determine the analyte concentration in a sample with composition between that of the two standards. Bertin (1964) and Fagel, Liebhafsky, and Zemaný (1958) used a binary-ratio method for the case in which only two elements are analyzed in a light matrix. Davis and Van Nordstrand (1954) used a set of calibration curves to determine the concentration of the analyte A as a function of some element B in the matrix.

Internal Standardization Method. The internal standardization method was first discussed by Hevesy and Alexander (1933), and later reviewed by Adler and Axelrod (1955). In this technique, a known amount of an element, which has a spectral line having excitation, absorption, and enhancement similar to those of the analyte line, is added to the sample as an internal standard, IS. The analytical concentration of the sample is then given by,

$$C_X = C_{IS} I_X / I_{IS} \cdot \quad (2.4)$$

The internal standard, IS, is usually an element having an atomic number one or two above or below that of the analyte. Many workers have applied, modified, refined, and extended this approach, as shown by the 24 cases listed by Müller (1972).

This method is used to compensate for long-term instrument drift and the matrix effects in many types of specimens. In particular, it partially compensates for variations in density in powders and briquet specimens. In liquids, it compensates for density, evaporation, and bubble formation. Often, it is not necessary to measure the background intensity, since it is substantially the same for the analyte, as well as for the internal standard, in which case the peak-intensity ratio is used. On the other hand, this method is not applicable to many types of samples, such as bulk solids, foils, and small fabricated parts; nor at high analyte concentrations (over 25%).

External-Standard Method. An external standard is a specimen from which some intensity value is measured to be ratioed with the

analyte-line intensity. The standard may be one of the samples retained for this purpose, or it may be any stable specimen not necessarily bearing any relation to the samples to be analyzed. Hirokawa (1962) used the emission lines from the specimen-mask plates of zinc or lead as external-standard lines in the analysis of impurities in steel. Lincoln and Davis (1959) used the analyte relative intensity in relation to an external standard to compensate for long-term drift in the spectrometer.

In general, the calibration standardization methods described above have been applied to compensate variations in volume, temperature, and density, as well as for the matrix or inter-element effects.

2.1.3 Standardization with Scattered X-Rays

The effect of the matrix on the fluorescent intensity may be compensated for by making use of the diffusely scattered x-rays, or background radiation. Andermann and Kemp (1958) were the first to show that the intensity of the diffusely scattered background intensity also depends upon the absorption characteristic of the matrix. They also demonstrated its great value in compensating absorption, density, and particle-size effects, as well as for instrumental drift. This method is especially suitable for low atomic number elements, as shown by Campbell and Thatcher (1962), Ryland (1964), and Reynolds (1963).

2.1.4 Dilution Methods

The dilution method for the analysis of multi-element mixtures is described extensively by Kemp, Hasler, and Jones (1954), Claisse (1957), Blavier et al. (1960), Wang (1962), Bruch (1962), and others.

This technique is used to correct for matrix effects by reducing the absorption characteristic of the matrix to a value determined by the diluent, and/or to correct for inhomogeneity and particle-size effects by dissolution during fusion of the sample. The diluents may be added in either or both of two ways: 1) a high concentration of a diluent of relatively very low absorption coefficient, such as borax ($\text{Na}_2\text{B}_4\text{O}_7$), lithium tetraborate (LiB_4O_7), and other fluxes; and 2) a low concentration of a diluent of high absorption coefficient, such as BaO , BaSO_4 , LaO_3 , or KSO_2 . In either case, the concentrations of the elements in the original sample are reduced to the extent that the concentrations are nearly proportional to the fluorescent intensities, since the absorption coefficient of the diluted specimen is largely determined by the diluent for both primary and analyte radiations. Dilution also minimizes enhancement, either by the reduction of the concentration of the enhancing element or by increasing the absorption of the enhancing spectral line. A heavy absorber is often added to reduce the matrix effects of the original matrix when a low absorption diluent such as BaO_2 or KClO_3 is used to reduce inhomogeneity or particle-size effects (Gunn, 1957).

2.1.5 Thin-Film Methods

The inter-element effects are substantially minimized in specimens that are very thin because neither primary nor secondary radiations are significantly absorbed in the thin layer. Since atoms absorb and emit independently of the other atoms present, the analyte-line intensity is directly proportional to the analyte concentration.

Rhodin (1955) developed the thin-film technique to analyze thin, metallic films of iron, chromium, and nickel. Andermann and Kemp (1958), by a careful calibration procedure, were able to measure film thickness in the range of 30 Å to 600 Å. Birks (1959) demonstrated that the inter-element effects disappear in a thin-film specimen, and Gunn (1961) developed a simple relation between analyte-line intensity and the number of analyte atoms in a thin film. Gunn also developed a technique to obtain thin films by evaporating a solution of the sample on a mylar film.

2.2 Mathematical Methods

The relationship between fluorescent intensity and concentration may also be expressed mathematically in the form of an equation, where a regression function is determined instead of a calibration curve. However, the parameters relating concentration and line intensity produce complex functions. Thus, many alternative correction procedures have been developed which are usually far easier to apply and frequently produce data which are at least as accurate as that obtained from more sophisticated methods. The mathematical methods which have been found most valuable in x-ray analysis may be divided into two distinct categories: 1) the influence coefficient method; and 2) the fundamental parameters method.

2.2.1 The Influence Coefficient Method

Determination of concentration in a multi-element mixture is best formulated mathematically as a linear system of equations. This system

of equations is derived by means of regression equations, with a unique equation being formulated for every component. The concentrations of the individual components are found by searching for such values and concentrations, respectively, for which the total system of equations is fulfilled simultaneously.

The first attempt at deriving working equations from first principles to relate measured analyte-line intensity and concentration was made by Glocker and Schreiber (1928), who derived a relationship for primary fluorescence only. Gillman and Heal (1952) formulated relationships that included secondary fluorescence effects.

The linear system of equations to determine a relationship between the measured intensity and concentrations (weight fractions) in a multi-element mixture was first attempted by Sherman (1954, 1955), and later used by Noakes (1954), Pluncherry (1963), Preis and Esenwin (1959), Burham, Howser, and Jones (1957), and others. The Sherman system of equations is obtained from the following,

$$(a_{ii} - t_i)C_i + \sum a_{ij}C_j = 0, \quad i \neq j; \text{ and} \quad (2.5)$$

$$\sum C_i = 1, \quad (2.5a)$$

where C_i is the concentration of element i , t is the counting time required to measure the analyte-line intensity, and a_{ij} is the influence coefficient of element j on i .

Beattie and Brissey (1954) analyzed a multi-element mixture by establishing linear simultaneous equations involving empirical absorption

coefficients, a_{ij} , involving the absorption coefficient of elements i and j only. The intensity and concentration are related as follows,

$$- (R_i - 1)C_i + \sum a_{ij}C_j = 0, \quad i \neq j, \quad (2.6)$$

where the influence coefficients, a_{ij} 's, are the quotients of the combined mass absorption coefficients for the primary tube radiation and the emerging analyte-line radiation,

$$a_{ij} = \frac{\mu(\lambda)_j}{\sin \phi} + \frac{\mu(\alpha)_j}{\sin \psi}, \quad (2.7)$$

where $\mu(\lambda)$ and $\mu(\alpha)$ are the mass absorption coefficients for the primary and secondary radiation, respectively. R_i is the relative intensity of analyte i with respect to a pure i standard; ϕ is the incidence angle; and ψ is the take off angle.

Birks (1959) derived a similar equation based on the following assumptions: 1) the specimen is homogeneous, infinitely thick, and has a flat surface; 2) the primary x-ray radiation is monochromatic; and 3) the enhancement effects have the same effect as low matrix absorption, or that enhancement can be regarded as negative absorption. As a first approximation, the absorption coefficients were obtained from intensity data of binary systems.

Alley and Myers (1965) applied a multiple regression analysis to derive regression coefficients that would account for the inter-element effects of the matrix. Mitchell and O'Hear (1966) applied a similar multiple regression analysis to study a series of metallic alloys, using a digital computer to solve the regression equations for the first time.

Criss and Birks (1968) applied a similar analysis to Birks's earlier work and obtained the following system of equations,

$$(R_i a_{ij} - 1) + \sum a_{ij} C_j = 0, \quad i \neq j, \quad (2.8)$$

to determine all of the coefficients simultaneously, from multi-element standards similar to the sample. This method corrects for the assumptions in the derivation of the system of equations given by Birks (1959).

Multiple regression analysis has also been applied by other workers using the following equations:

1. Burham, Howser, and Jones (1957),

$$(a_{ii} - t_i) C_i + \sum a_{ij} C_j = 0, \quad i \neq j; \quad (2.9)$$

2. Guinier (1961),

$$R_i = C_i / (C_i + \sum a_{ij} C_j) = 0, \quad i \neq j; \quad (2.10)$$

3. Lucas-Tooth and Price (1961),

$$C_i = a_i + l_i (b + \sum a_{ij} l_j); \quad (2.11)$$

4. Lachance and Traill (1966),

$$R_i = C_i / (1 + \sum a_{ij} C_j), \quad i \neq j; \quad (2.12)$$

5. Claisse and Quintin (1967),

$$C_i / R_i = 1 + \sum_{j \neq i} a_{ij} C_j + \sum_{k \neq i} \sum_{j \neq i} B_{ikj} C_k C_j; \quad \text{and} \quad (2.13)$$

6. Rasberry and Heinrich (1974),

$$C_i/R_i = 1 + \sum_{i \neq j} A_{ij}C_j + \sum_{i \neq j} B_{ij}C_j/(1 + C_i) , \quad (2.14)$$

where C is concentration (weight fraction); R_i is the relative intensity of analyte i with respect to some standard; a_{ij} 's are the influence coefficients of element j on i ; and A_{ij} and B_{ij} are absorption and enhancement influence coefficients, respectively.

The influence coefficients method has some difficulties that can be ascribed to the following: 1) the empirical coefficients are derived on the assumption that the primary x-ray radiation is monochromatic; 2) enhancement by secondary radiation occurring within the sample has the same effect as low matrix absorption; and 3) a large number of standards is required by some methods to determine the influence coefficient.

2.2.2 The Fundamental Parameters Method

The fundamental parameters method is based on the assumptions that the specimen is homogeneous, very thick in comparison to the penetration depth of the x-ray radiation (0.1 to 0.003 mm) (Koh and Caugherty, 1952), and has a reasonably flat surface. In this method, the measured intensity is converted to analytical composition by entirely mathematical means, and without intermediate standards or empirical coefficients. This method does, however, require the knowledge of the spectral distribution of the primary radiation, the mass absorption coefficients as functions of wavelength, and the fluorescent yields. Unfortunately, the calculations are extremely complex, only limited success has been obtained,

and the method is appropriate only for simple systems. Therefore, an iteration process must be used to determine the analytical concentrations, in which successively better estimates of the concentrations are made until the calculated intensities from the fundamental parameters equations agree with the measured intensities (Birks, 1959).

The intensity formula based on fundamental parameters was first derived by Hamos (1945), and later discussed by Sherman (1954), Gillman and Heal (1952), and by Shiraiwa and Fujino (1966). It was not until Gilfrich and Birks (1968) determined the real spectral intensity distribution for W, Mo, and Cr x-ray tubes that it was possible for Criss and Birks (1968) to calculate the exact fluorescence intensity regarding primary and secondary fluorescence due to polychromatic radiation. Probably the most successful approach to the use of fundamental data for the evaluation of concentrations from measured intensities is the method of Criss and Birks (1968), where the primary and secondary radiation intensities are given by the following:

1. Primary intensity,

$$I(\lambda)_p = G_i C_i \sum \frac{D_{ip} \mu_{ip} I_p \Delta \lambda}{\mu_{mp} / \sin \phi_1 + \mu_{mi} / \sin \phi_2} ; \text{ and} \quad (2.15)$$

2. Secondary intensity,

$$\begin{aligned}
 I(i)_s = G_i C_i \sum_j \left\{ \frac{1}{\mu_{ip}} \sum_j D_{jp} C_j K_j \mu_{ij} \mu_{jp} \right. \\
 \cdot \left[\frac{1}{\mu_{mp} \csc \phi_1} \text{Ln} \left(1 + \frac{\mu_{mp} \csc \phi_1}{\mu_{mj}} \right) \right. \\
 \left. \left. + \frac{1}{\mu_{mi} \csc \phi_2} \text{Ln} \left(1 + \frac{\mu_{mi} \csc \phi_2}{\mu_{mj}} \right) \right] \right\}, \text{ and } \quad (2.16)
 \end{aligned}$$

$$R_i = [I(\lambda)_p + I(i)_s] / I(\lambda)_{ii}, \quad (2.17)$$

where R_i is the relative intensity; μ_{mp} , μ_{mi} , μ_{ip} , and μ_{ij} are the mass absorption coefficients for primary and analyte-line radiations; D_{ip} is a constant of zero or unity value depending on whether or not the particular primary radiation can excite analyte i ; K_i is the probability of emission of a particular spectral series; and G_i is the probability of emission of a particular spectral line.

Although the method is theoretically correct, since the matrix absorption and analyte excitation by the matrix are considered explicitly for each element in the specimen, there are certain limitations to its applications. The following are some of the principal limitations:

1) the present uncertainty associated with the mass absorption coefficients and the fluorescent yields; and 2) the complexity of the calculations involved.

2.2.3 Simulation Techniques

The probabilistic Monte Carlo method has been applied by Green (1963), Archard and Mulvey (1963), Bishop (1965), and Birks, Ellis, and Grant (1966) in quantitative x-ray emission microanalysis to determine the distribution of x-rays within a pure target when excited with an electron source. This technique utilizes a finely focused electron beam to excite the sample, and the x-rays produced within the sample are then recorded by a spectrometer. Recently, Gardner and Hawthorne (1975) applied the Monte Carlo method to calculate the intensity of x-ray secondary emission in a system excited by gamma rays from a radioactive source. Although it has been applied to simulate other particle processes, it has not yet been applied to x-ray fluorescence spectroscopy.

CHAPTER 3

SIMULATION TECHNIQUE

A Monte Carlo model was developed to simulate the x-ray fluorescence process and to study the inter-element effects within a homogeneous multi-element mixture. The model was simulated with the aid of a computer program developed on the x-ray principles set forth in the following paragraphs.

In quantitative x-ray spectrometric analysis, it is the analyte line intensity that is measured and used to determine the analyte concentration. The emitted intensity is affected by: 1) the spectral distribution of the primary x-ray beam; 2) the absorption of the primary x-rays by both the analyte and the matrix; 3) the excitation probability and the fluorescent yield of the analyte line; 4) the absorption of the analyte line by the analyte and the matrix; and 5) the geometry of the x-ray spectrometer.

To understand the model, consider the process of secondary excitation of an analyte line in a homogeneous multi-element mixture.

In Fig. 3.1, consider an incremental layer of thickness dx , at a depth x , in a specimen of density ρ . The incident angle of the primary x-rays is ϕ , and the take-off angle of the analyte-line beam is ψ . The intensity of the primary x-ray beam that could excite the analyte line is that portion of the x-ray tube spectral distribution between the

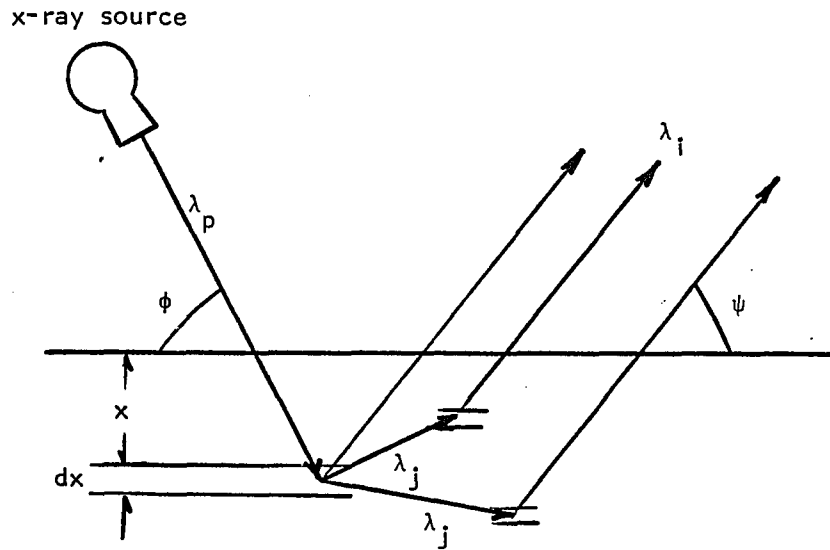


Fig. 3.1 Secondary Emission of Element i , Excited by the Primary X-Ray Beam, and Element j Radiation.

short-wavelength limit of the tube, λ_{swl} , and the analyte-line absorption-edge wavelength, λ_{abs} ,

$$I_o = \int_{\lambda_{swl}}^{\lambda_{abs}} I_o(\lambda) d\lambda . \quad (3.1)$$

The incremental loss in intensity, dI , of radiation passing through an incremental layer, dx , is proportional to the initial intensity of the primary x-rays, I_o (Fig. 3.2),

$$dI_x \propto - I_o dx . \quad (3.2)$$

The constant of proportionality is called the linear absorption coefficient and is usually written as μ_x . Rewriting and integrating over the limits in Fig. 3.2,

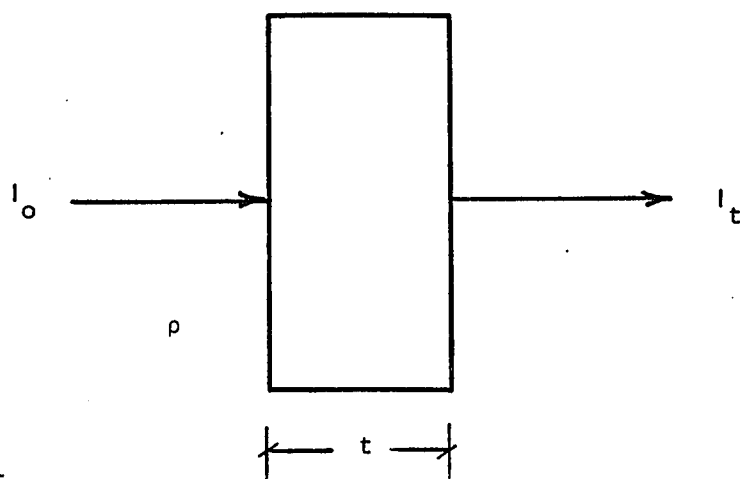
$$dI_x/I_o = - \mu_x dx \quad (3.3)$$

$$I_t/I_o = \exp (- \mu_x t) \quad (3.4)$$

A more significant and useful parameter in x-rays is the mass absorption coefficient which is related to the density as follows,

$$\mu_m = \mu_x/\rho \quad (\text{cm}^2/\text{g}) , \quad (3.5)$$

where μ_x is the linear absorption coefficient and ρ is the density. Throughout this work, μ will refer to the mass absorption coefficient unless otherwise indicated.



$$I_t/I_0 = \exp(-\mu t)$$

Fig. 3.2 Absorption through a Slab of Thickness t .

The attenuation of the primary beam in reaching dx is,

$$I_x(\lambda, x)d\lambda = I_o(\lambda)d\lambda \exp [-\mu_M(\lambda)x\rho/\sin \phi] , \quad (3.6)$$

where $\mu_M(\lambda)$ is the weighted average absorption coefficient of the matrix, M , for the given wavelength,

$$\mu_M(\lambda) = \Sigma C_i \mu_i(\lambda) , \quad (3.7)$$

where C_i is the weight fraction of element i in the matrix.

Of the photons absorbed by the entire matrix, the fraction absorbed by the analyte, A , having concentration C_a , and mass absorption $\mu_a(\lambda)$ is

$$C_a \mu_a / \mu_M(\lambda) . \quad (3.8)$$

Then, only a certain fraction of the photons absorbed by the analyte will contribute to excite the atom shell corresponding to the series of the analyte line; for example, K shell. This fraction is related to the absorption-edge jump ratio of the analyte for that shell, r_K , and is given by,

$$(r_K - 1)/r_K , \quad (3.9)$$

where r_K is defined as the ratio of the mass absorption coefficient evaluated at the short- and long-wavelength sides, as given by,

$$r_K = \frac{\mu_K + \mu_{L1} + \mu_{L2} + \mu_{L3} + \dots}{\mu_{L1} + \mu_{L2} + \mu_{L3} + \mu_M + \dots} , \quad (3.10)$$

where the μ_i 's are the mass absorption coefficients of the analyte evaluated at the different absorption-edge wavelengths.

When the atom is ionized in one of the inner shells, an electron from an outer shell transfers into the vacancy and, in the process, emits radiation of an energy corresponding to the energy difference between the two shells. This energy may be released as a characteristic or secondary photon, in which case the process is x-ray fluorescence or secondary emission. On the other hand, the released energy may be absorbed by the atom itself, ejecting an electron from an outer shell, which is called radiationless transition or Auger emission.

Therefore, only a fraction of all the electron transitions will result in characteristic or secondary emission and is defined as the fluorescent yield, ω , which is the fraction of all electron transitions, n , which are associated with the emission of secondary photons, n_K ,

$$\omega_K = n_K/n . \quad (3.11)$$

Furthermore, of the fraction of K photons emitted, the fraction that leads to emission of the particular analyte line, K-alpha, to be measured is given by the probability of the orbital transition resulting in that line, g_K .

The intensity of the analyte line produced in the layer dx by the primary beam is given by,

$$dI(\lambda, x)_\alpha = I_0(\lambda, x) d\lambda \frac{E_a C_a \mu_a(\lambda)}{\mu_M(\lambda)} \rho \frac{dx}{\sin \phi} , \quad (3.12)$$

where E_a may be defined as a probability of emission,

$$E_a = (1 - 1/r_K) \omega_K g_K . \quad (3.13)$$

Since x-ray fluorescence is emitted uniformly in all directions, only a fraction, q , which is a function of the instrument geometry, will be intercepted by the optical system of the spectrometer. As it emerges from the specimen, the analyte-line radiation is attenuated by the matrix by the factor,

$$\exp (- \mu_M(\lambda) x \rho / \sin \psi) . \quad (3.14)$$

The characteristic radiation is produced at all depths, x , and by all the wavelengths between the short-wavelength limit of the spectrum of the x-ray tube and the analyte absorption edge. Then, the analyte-line intensity is given by,

$$I_a = \frac{q E_a C_a}{\sin \phi} \int_{\lambda_{swl}}^{\lambda_{abs,a}} \mu_a(\lambda) \rho I_o(\lambda) d\lambda \cdot \int_x^t \exp \left\{ - x \rho \left[\frac{\mu_M(\lambda)}{\sin \phi} + \frac{\mu_M(a)}{\sin \psi} \right] \right\} dx \quad (3.15)$$

For a very thick specimen, where the thickness is very large as compared to the penetration depth of the x-rays, Equation (3.15) becomes

$$I_a = \frac{q E_a C_a}{\sin \phi} \int_{\lambda_{swl}}^{\lambda_{abs,a}} \frac{\mu_a(\lambda) I_o(\lambda) d\lambda}{\frac{\mu_M(\lambda)}{\sin \phi} + \frac{\mu_M(\lambda)}{\sin \psi}} . \quad (3.16)$$

The fluorescent intensity, which is excited by the spectral lines of one or more of the matrix elements, has been derived following a similar analysis by Gillman and Heal (1952), Sherman (1955), Renaud (1963), Shiraiwa and Fujino (1966), and is given by the following equation,

$$I_{a,j} = \frac{qE_a C_a E_j C_j}{\sin \phi} \int_{\lambda_{swl}}^{\lambda_{abs,j}} \frac{\mu_a(j) \mu_j(\lambda) I_o(\lambda) L d\lambda}{\frac{\mu_M(\lambda)}{\sin \phi} + \frac{\mu_M(j)}{\sin \psi}}, \quad (3.17)$$

$$L = \frac{\text{Ln} \left[1 + \frac{\mu_M(\lambda)}{\mu_M(j) \sin \phi} \right]}{\mu_M(\lambda)/\sin \phi} + \frac{\text{Ln} \left[1 + \frac{\mu_M(a)}{\mu_M(a) \sin \psi} \right]}{\mu_M(a)/\sin \psi},$$

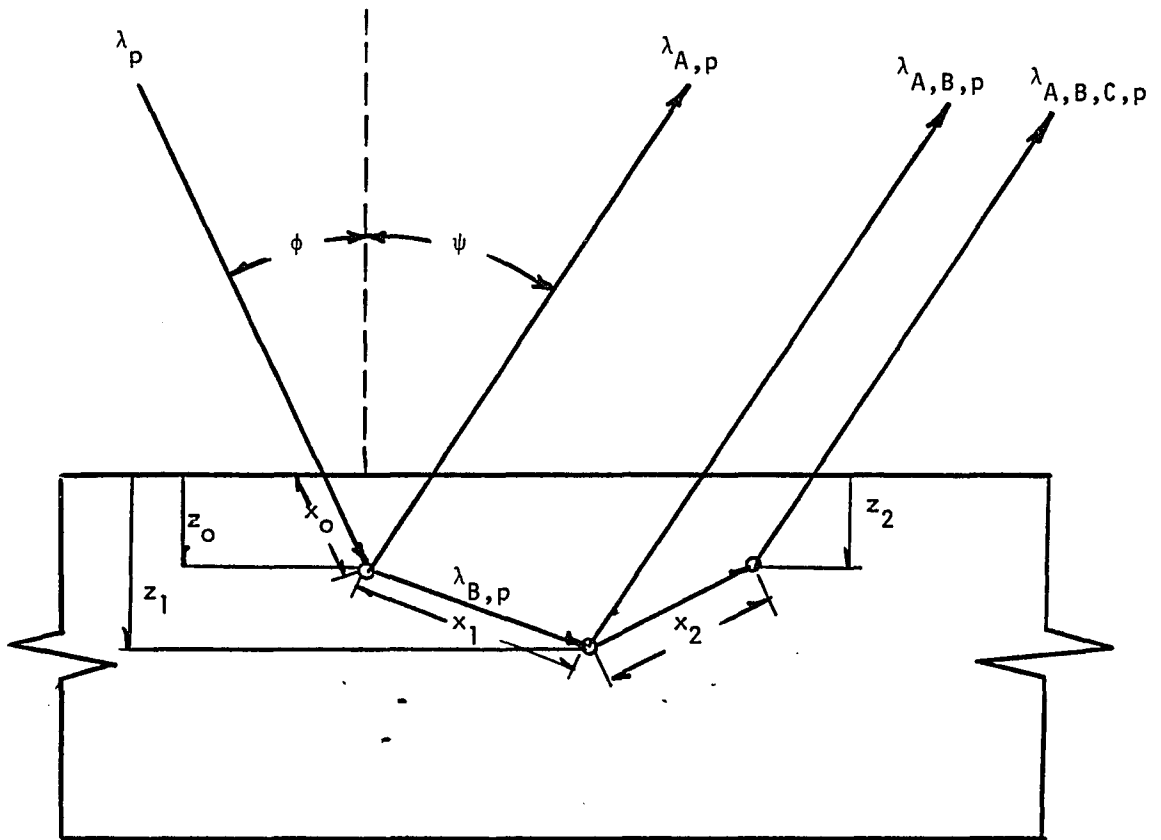
where $I_{a,j}$ is the contribution of element j to the analyte-line intensity. The total analyte-line intensity, then, is given by

$$I_a = I_{a,p} + \sum I_{a,j}. \quad (3.18)$$

The analyte-line intensity due to indirect enhancement or tertiary effect, which occurs when the primary x-ray tube radiation excites an element in the matrix, which in turn excites a second element whose characteristic radiation is strong enough to excite the analyte, has been reported by Sherman (1955) and Shiraiwa and Fujino (1966).

3.1 Derivation of the Monte Carlo Model

The system to be treated is illustrated in Fig. 3.3; it consists of a homogeneous, infinitely thick, multi-element specimen. It is further assumed that it is excited with polychromatic x-rays.



ϕ = angle of incidence
 ψ = take-off angle
 x = free path
 z = collision coordinate

Fig. 3.3 X-Ray Fluorescence Model.

Since each event of the x-ray fluorescence process is independent of each other and governed by probability functions, a random probability may be assigned to each event; then this probability is compared with some pre-assigned probability distribution function to determine the outcome of the event. In our case, a photon is emitted with a random energy chosen from the probability distribution function (PDF) of the energy source, and the distance traveled without an interaction is played for. Then one must determine the matrix atom that will undergo some interaction with the photon. After the colliding atom is determined, the type of interaction must be determined or played for; it could be absorption or scattering. If the photon is absorbed, the type of emission is played for according to the emission pre-assigned probability; it could be characteristic radiation or Auger emission. If characteristic radiation occurs, then one must play for the particular line emission, K-alpha or K-beta. If the photon was scattered, a similar procedure as for absorption is followed to determine the type of scattering, elastic or inelastic. For the new secondary photon emitted or for the scattered photon, a direction is then assigned from the PDF governing that event. A record is maintained of the outcome of all the events involved in each photon path history, and updated with each interaction.

The aim of the simulation is to trace a sufficiently large number of photon trajectories to allow an approximation to the conditions that exist in a real sample.

3.1.1 Random Wavelength Source

The intensity distribution of the continuous spectrum can be expressed as follows (Kramers, 1923),

$$I(\lambda)d\lambda = KiZ \left[\frac{\lambda^{-1}}{\lambda_{sw1}} - \lambda^{-2} \right] d\lambda , \quad (3.19)$$

where K is a constant, Z is the target's atomic number, i is the applied current, and λ_{sw1} is the short-wavelength limit associated with the maximum energy of the exciting primary electrons.

If the probability density function, $P(\lambda)$, is defined as follows,

$$P(\lambda) = I(\lambda) / \int_{\lambda_1}^{\lambda_2} I(\lambda)d\lambda , \quad (3.20)$$

and the corresponding cumulative probability density function as,

$$R(\lambda) = \int_{\lambda_1}^{\lambda_2} P(\lambda)d\lambda = r , \quad (3.21)$$

the value of λ is determined uniquely as a function of r . Moreover, if r is a random number uniformly distributed on $0 \leq r \leq 1$, then λ falls with frequency $I(\lambda)d\lambda$ in the interval (λ_1, λ_2) .

Therefore, for the wavelength interval of interest, $\lambda_{sw1} \leq \lambda \leq \lambda_{abs}$, then Equation (3.21) becomes,

$$r = \frac{\left[\frac{1}{\lambda_{swl}} \ln \frac{\lambda}{\lambda_{swl}} + \left(\lambda^{-1} - \lambda_{swl}^{-1} \right) \right]}{\left[\frac{1}{\lambda_{swl}} \ln \frac{\lambda_{abs}}{\lambda_{swl}} + \left(\lambda_{abs}^{-1} - \lambda_{swl}^{-1} \right) \right]} \quad (3.22)$$

If a large number of random numbers is chosen, and this equations is solved for λ each time, the computing time will become too large for practical calculations. To avoid this difficulty, Equation (3.22) is numerically solved over the given wavelength range, and fit by means of a least-squares polynomial to an m-degree polynomial of the form,

$$\lambda = a_0 + a_1 r + a_2 r^2 + a_3 r^3 + \dots + a_m r^m . \quad (3.23)$$

Then, for a given value of r , the wavelength of the primary photon can be determined, and all the program parameters and x-ray properties that depend on the wavelength can be calculated.

3.1.2 Length of the Free Path

The distance traveled by a photon between interactions is known as the free path, and it is a random variable.

The fraction of the incident energy absorbed by the matrix at a distance x may be defined as the probability, $p(x)$, that a photon can move through a distance x without undergoing a collision,

$$p(x) = \exp (- \mu_x x) . \quad (3.24)$$

Therefore, the probability that a photon can move through a distance x and then undergo a collision at dx in the neighborhood of x is

$$p(x) = \exp(-\mu_x x) \mu_x dx, \quad (3.25)$$

and the corresponding probability distribution function is

$$p(x) = \int_0^x \mu_x \exp(-\mu_x x) dx, \quad (3.26)$$

$$= 1 - \exp(-\mu_x x). \quad (3.26a)$$

The average distance, \bar{x} , between collisions is known as the mean free path, and for a homogeneous specimen is given by,

$$\bar{x} = \int_0^{\infty} \mu_x x \exp(-\mu_x x) dx = 1/\mu_x. \quad (3.27)$$

It follows that the random free path must be expressed as,

$$r = p(x) = 1 - \exp(-x/\bar{x}), \quad (3.28)$$

or,

$$x = \bar{x} \ln(1 - r). \quad (3.29)$$

Since $(1 - r)$ is uniformly distributed on $0 \leq r \leq 1$, the free path may then be played for according to,

$$x = -\ln r / \mu_x, \quad (3.30)$$

where μ_x is the linear absorption coefficient of the matrix.

3.1.3 The Colliding Atom

In the event of a collision of a photon in a homogeneous medium that contains different species, the probabilities of collision are proportional to the amounts of the various atoms present and to their mass absorption coefficients. If the photon is forced to interact within the sample, since the thickness is very large as compared to the penetration depth of the photon, then the probability of a collision with a given atom will be given by,

$$C_i \mu_i / \sum C_i \mu_i , \quad (3.31)$$

where C is the concentration (weight fraction), and μ is the mass absorption coefficient of the species. The colliding atom is played for by means of the scheme outlined below.

Consider a sample containing elements A, B, and C, with probabilities of collision, P_a , P_b , and P_c , respectively, which are the length of the intervals in Fig. 3.4.



Fig. 3.4 Probability Distribution Analogy.

In order to play for the colliding atom, a random number is generated and tested to determine in which interval it falls. If

$$r < P_a ,$$

the photon will collide with an atom of element A. If

$$P_a \leq r < (P_a + P_b) ,$$

then the collision will be with a B atom; and finally, if

$$(P_a + P_b) < r ,$$

the photon will collide with a C atom.

This technique or scheme to determine the outcome of a given event is to be applied throughout the simulation process to determine such events as the type of collision, type of emission, etc.

3.1.4 Sample Interactions

In x-ray fluorescence analysis, only scattering and photo-electric absorption must be considered. The ratios of the absorption and scattering coefficients to the total mass absorption coefficient characterize the probabilities of scattering and photo-electric absorption, respectively. These probabilities are used to determine the type of collision when the path history of the photon is being considered.

When a photon collides with an atom for which

$$\mu = \tau + \sigma_E + \sigma_I , \quad (3.32)$$

then the probabilities of photo-electric absorption, elastic and inelastic scattering are given by the following relations,

$$\tau/\mu ; \sigma_E/\mu ; \sigma_I/\mu . \quad (3.33)$$

The type of collision is played for by means of the scheme discussed in Section 3.1.3.

3.1.5 Secondary Emission

In order to determine if an absorption event will yield the desired analyte line, the probabilities of ionization, fluorescence, and emission must be defined. These probabilities are related to the absorption-edge jump ratio, r_K ; the fluorescent yield, ω_K ; and the probability of orbital transition resulting in the desired analyte line, g .

Thus,

$$\text{Probability of ionization} = (r_K - 1)/r_K , \quad (3.34)$$

$$\text{Probability of fluorescence} = \omega_K , \text{ and} \quad (3.35)$$

$$\text{Probability of K emission} = g_{K_\alpha} , \quad (3.36)$$

where g may be defined as the fractional value or relative intensity of the analyte line in its series. For example, the fraction of the total K-series x-ray photons emitted by the analyte that are K-alpha photons,

$$g_{K\alpha} = \frac{I_{K\alpha 1} + I_{K\alpha 2}}{\sum I_K} \quad (3.37)$$

where $\sum I_K$ is the sum of the intensities of all the analyte K-lines.

3.1.6 Scattering

If the photon is scattered by the matrix, then one must play for the type of scattering, elastic or inelastic. In elastic scattering, no change in wavelength or energy is involved. Therefore, if it is assumed that it is isotropic, the scattering direction may be played for from Equation (3.41).

If the scattering is inelastic, the incident photon is deflected with a corresponding change in wavelength, or energy loss. The change in wavelength is given by (Compton and Allison, 1935),

$$\Delta\lambda = 0.02426 (1 - \cos \theta) . \quad (3.38)$$

Hence, the scattering wavelength is determined from the following relation,

$$\lambda_s = \lambda_o + 0.02426 (1 - \cos \theta) , \quad (3.39)$$

where θ is the angle of scattering (Fig. 3.5).

3.1.7 Emission or Scattering Direction

X-ray secondary emission, as well as scattering, may be considered isotropic, uniformly distributed in all directions. In terms of spherical coordinates (θ , the polar angle; ϕ , the azimuthal angle;

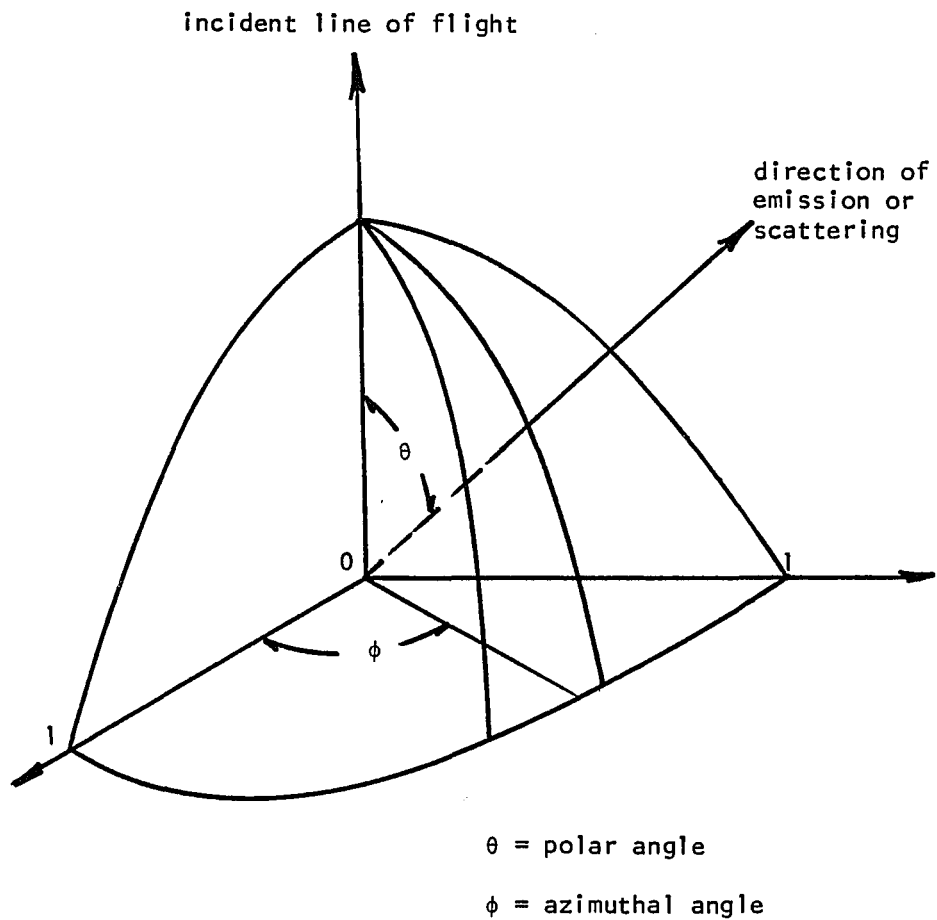


Fig. 3.5 Spherical Coordinates System for the Emission or Scattering Direction.

Fig. 3.5), we may choose a direction of emission or scattering from the following relations,

$$\int_0^\theta \sin \theta \, d\theta / \int_0^\pi \sin \theta \, d\theta = r , \quad (3.40)$$

or

$$\cos \theta = 1 - 2r , \quad (3.41)$$

and

$$\int_0^\phi d\phi / \int_0^{2\pi} d\phi = r , \quad (3.42)$$

or

$$\phi = 2\pi r . \quad (3.43)$$

3.1.8 Collision Coordinate

The collision coordinate is determined statistically from

$$Y_n = Y_{n-1} + x \cos \theta , \quad (3.44)$$

where x is the free path, n represents the number of collisions, and $\cos \theta$ is the direction of flight. This coordinate is used to determine if the collision occurs within the specimen, or if the photon emerges from the sample.

3.2 Description of the Flow Chart

The flow chart for the Monte Carlo simulation is illustrated in Fig. 3.6. See Appendix A for a complete listing of the actual program, PROGRAM X-RAYS, used in this investigation.

The following is a description of the program, step by step:

1. Box 1: input all the information needed to determine the program to be run.
2. Box 2: DO loop for repeating the program for different samples, or sets of concentrations. Once completed, STOP.
3. Box 3: read sample concentrations.
4. Box 4: preliminary calculations to determine the matrix density, absorption-edge jump ratios, atomic percentages, and other constants.
5. Box 5: print data and x-ray properties.
6. Box 6: initialize counters.
7. Box 7: DO loop for the specified number of photons to be tested; when completed, move to Box 56.
8. Box 8: generate random number and determine random wavelength.
9. Boxes 9, 10, and 11: the wavelength is tested to determine if it could excite the elements present, and activate the primary photons counter for each element.
10. Box 12: auxiliary calculations -- initial indices are set, and constant parameters are calculated.

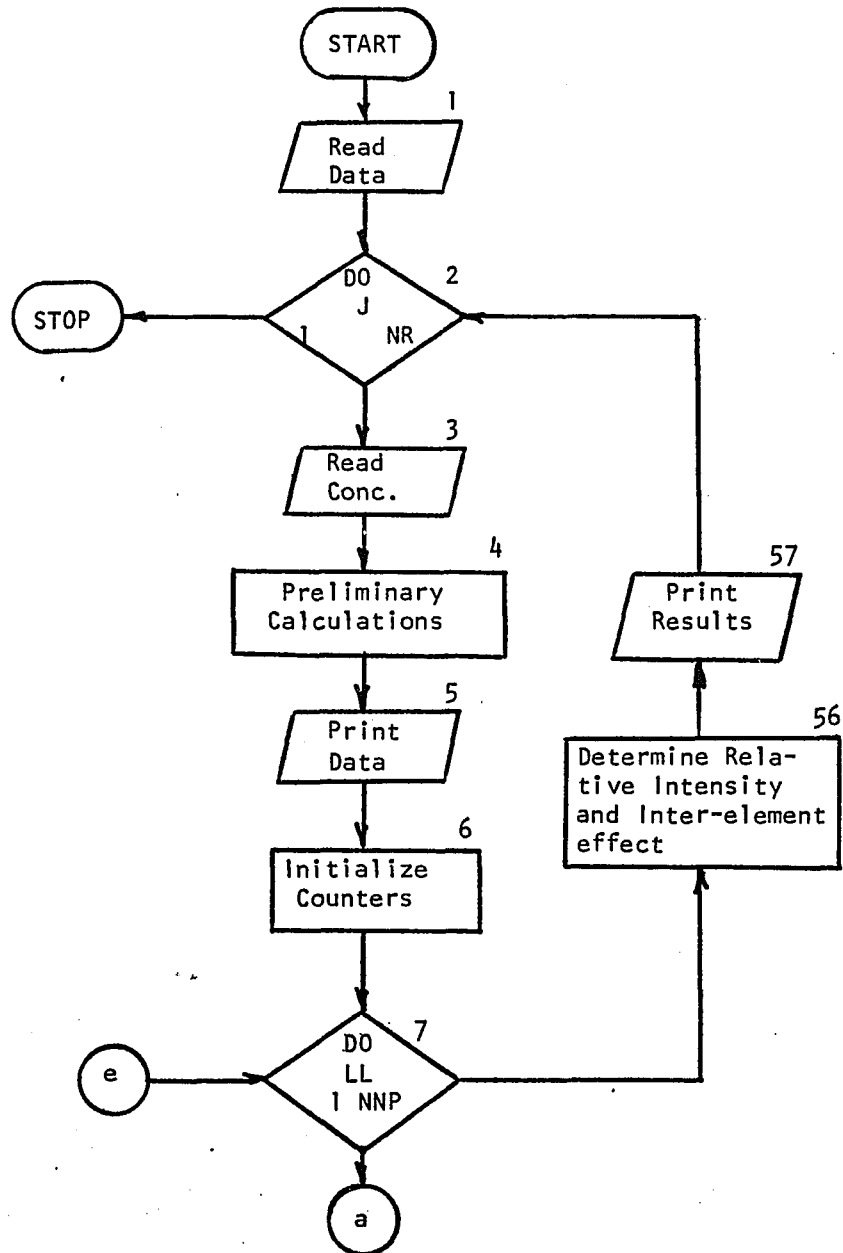


Fig. 3.6 Flow Chart for Program X-RAYS.

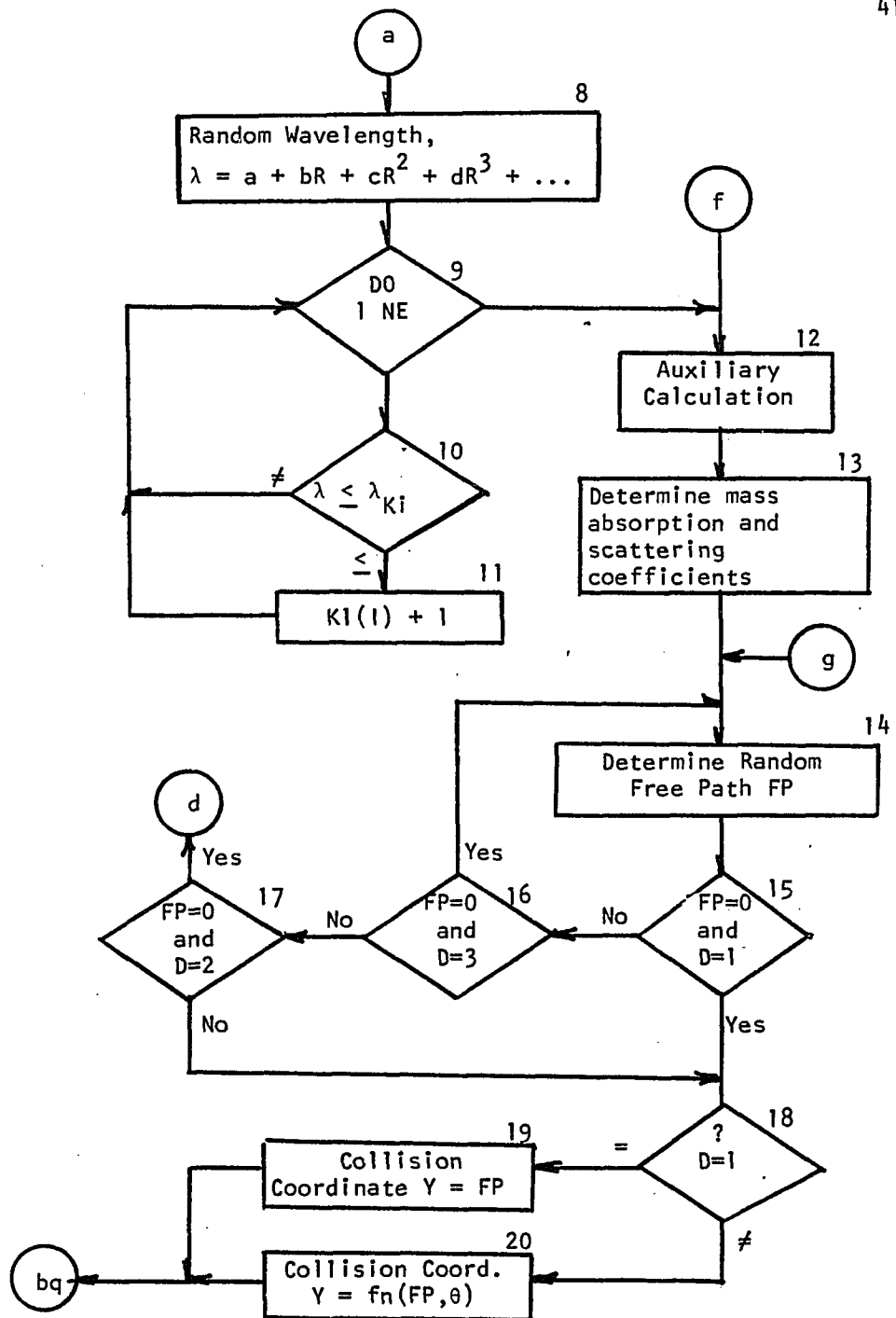


Fig. 3.6 Flow Chart, Continued.

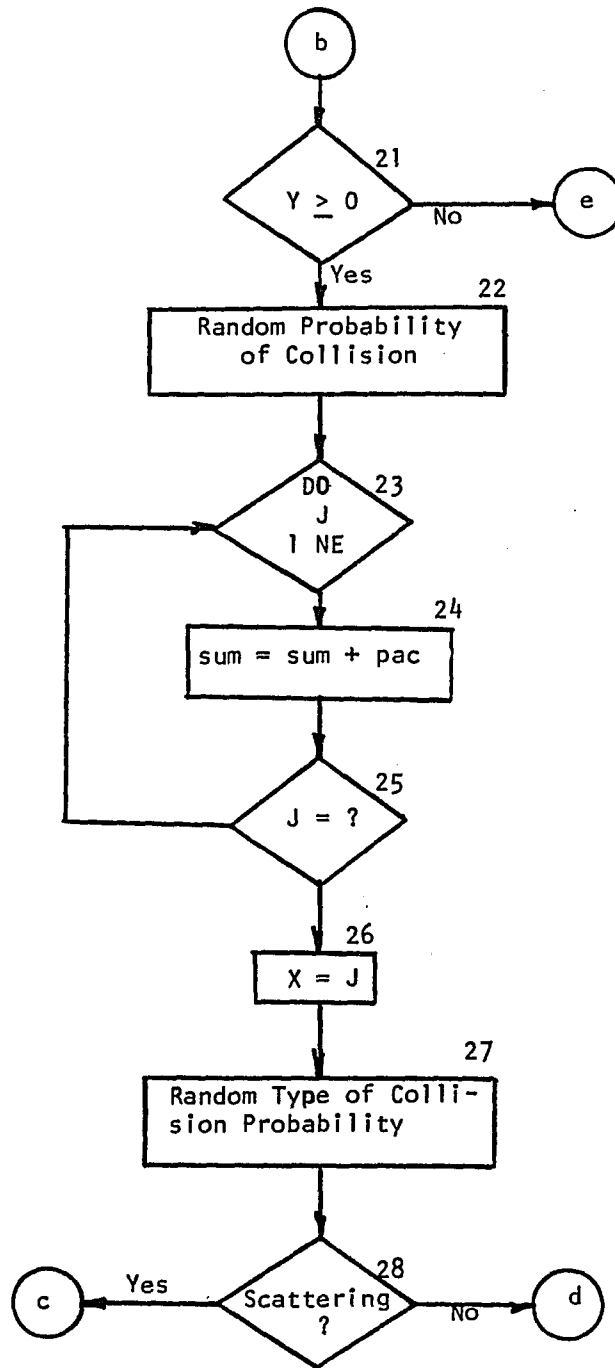


Fig. 3.6 Flow Chart, Continued.

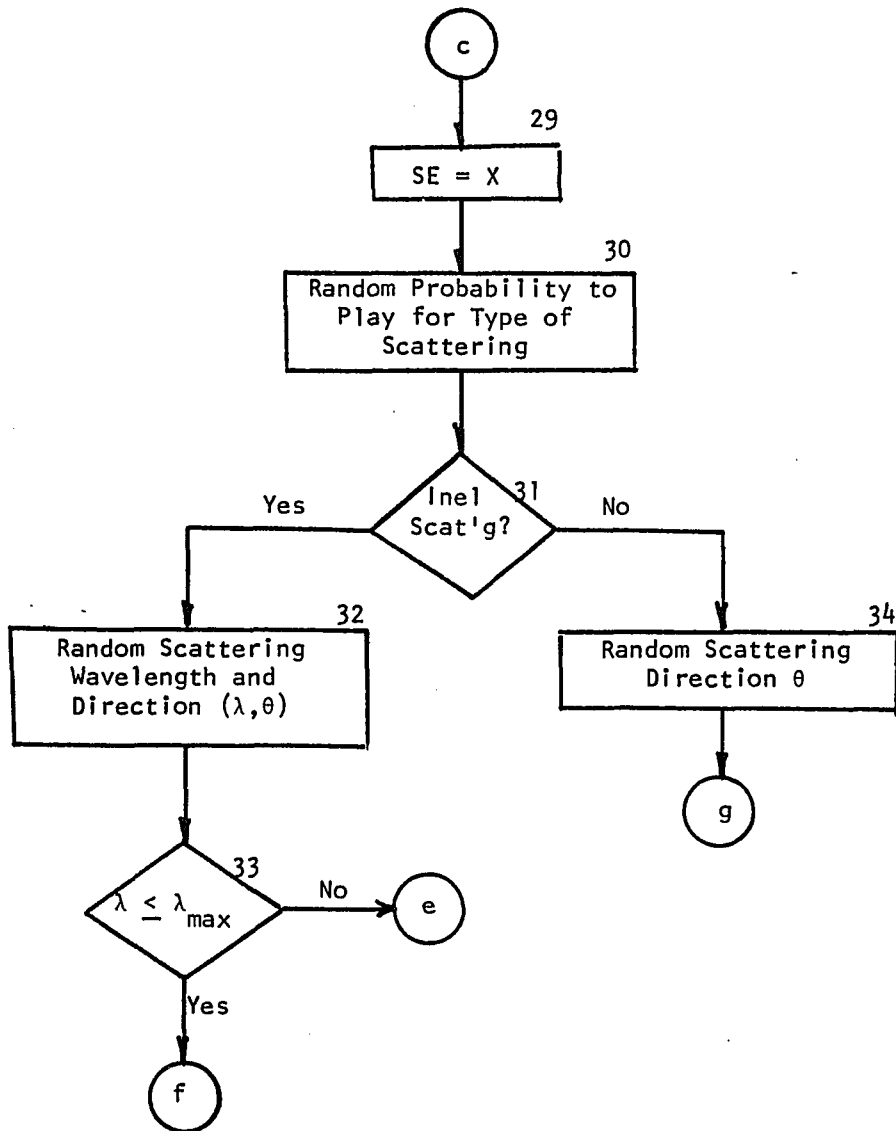


Fig. 3.6 Flow Chart, Continued.

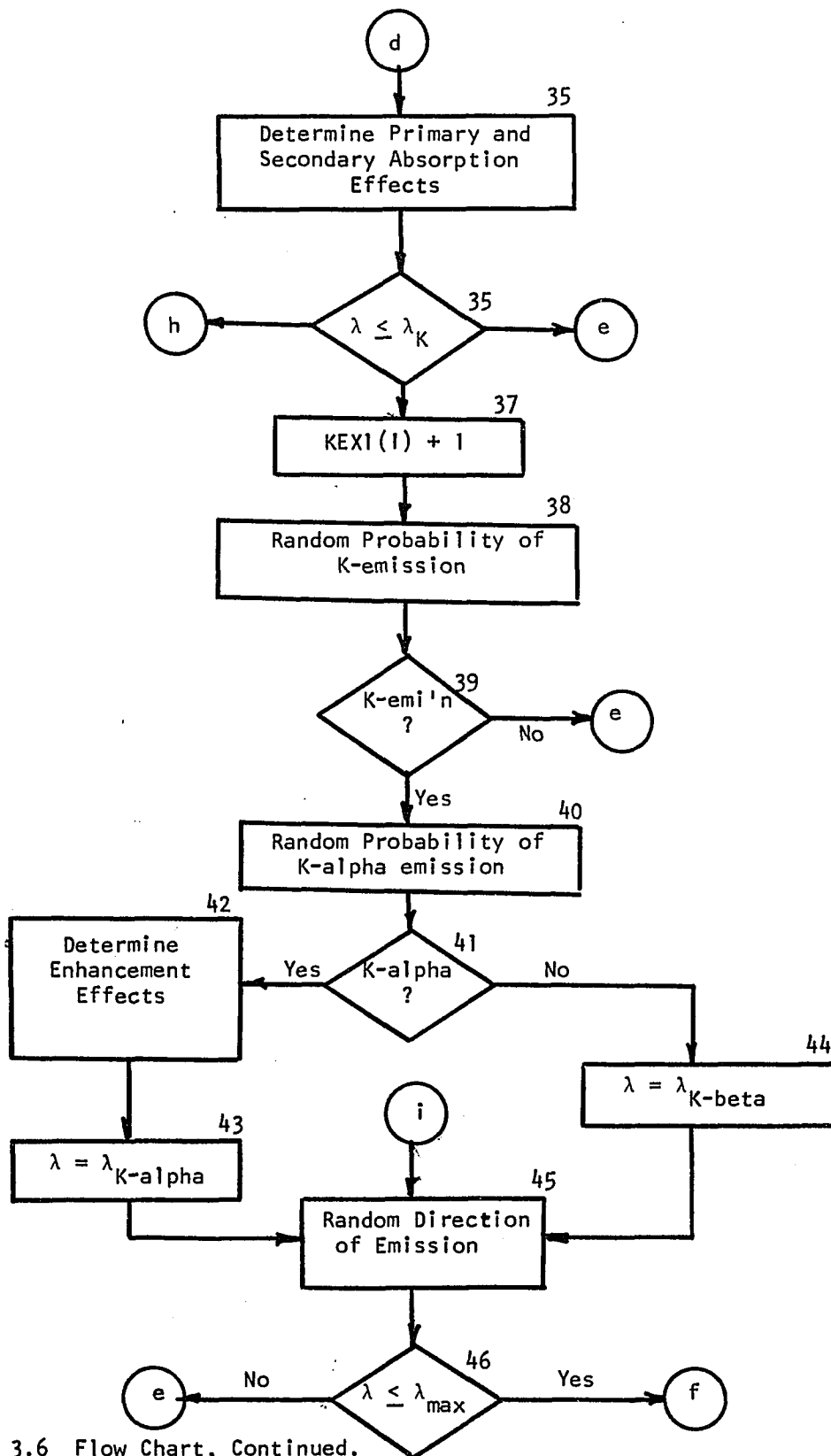


Fig. 3.6 Flow Chart, Continued.

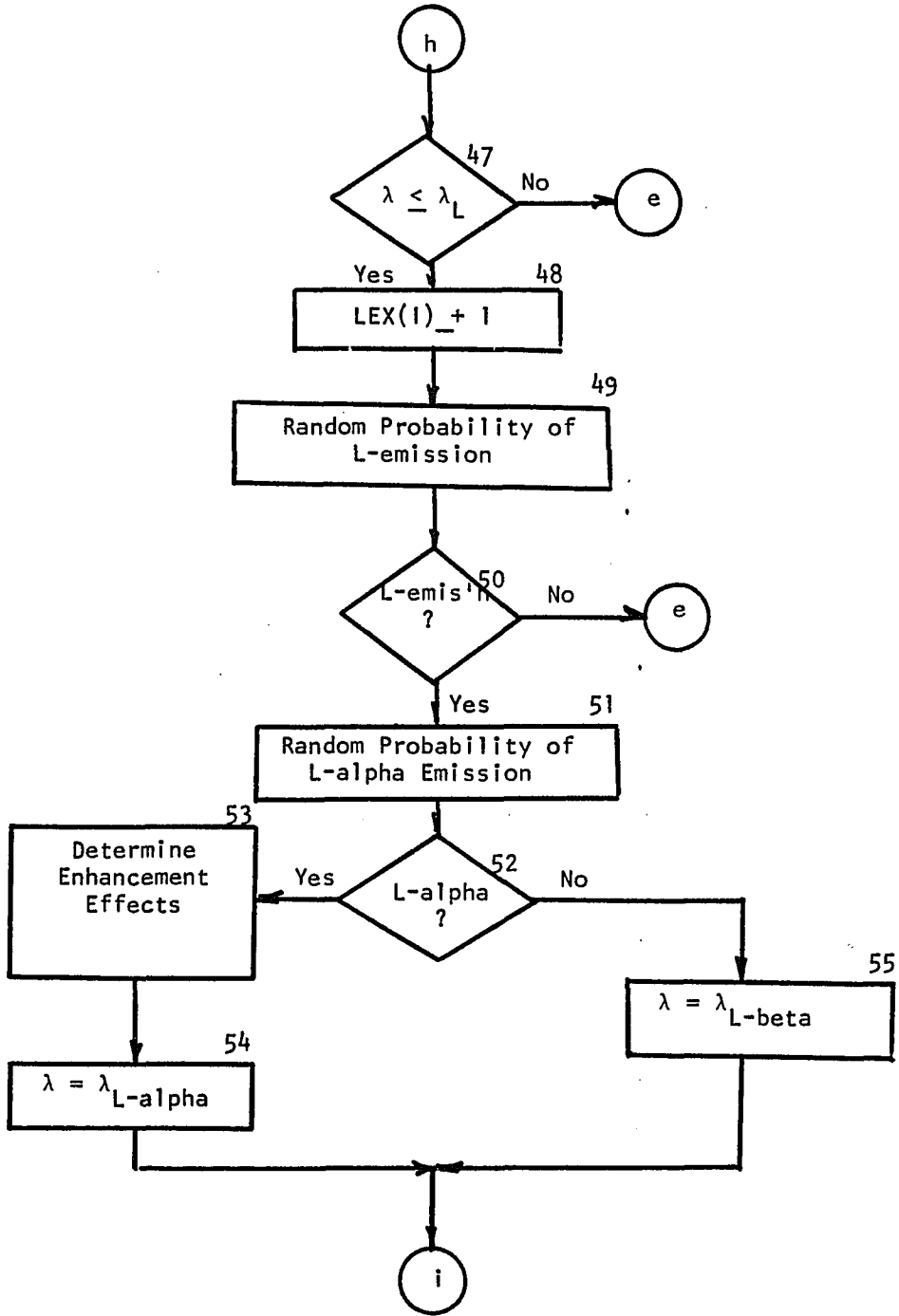


Fig. 3.6 Flow Chart, Continued.

11. Box 13: the mass absorption and scattering coefficients are calculated for every wavelength. Also, the corresponding probabilities are determined.
12. Box 14: generate random number and play for the random free path.
13. Boxes 15, 16, and 17: test the condition the free path is zero; if a primary photon, $D = 1$, the collision occurs at the surface and the program continues; if a secondary photon, $D = 2$, is recorded as self-absorption, and the program continues; and if $D = 3$, scattered photon, value is rejected and a new value is played for.
14. Boxes 18, 19, and 20: the penetration depth is determined; if a primary photon, the penetration is calculated from the free path and the angle of incidence; if a scattered or secondary photon, $D \neq 1$, then the penetration is determined from the free path and the scattering or emission direction.
15. Box 21: the collision coordinate is tested to determine if photon will interact within the specimen, or if it will emerge. If the photon emerges, path is ended and a new primary photon is generated, otherwise, program continues.
16. Box 22: generate random number and determine the random probability of collision, and play for the colliding atom.
17. Boxes 23, 24, and 25: this DO loop determines the colliding atom.

18. Box 26: the colliding atom is designated as X for future reference.
19. Box 27: generate a random number and determine the probability of scattering.
20. Box 28: test to determine the type of collision; if absorption, go to Box 35, otherwise go to Box 29.
21. Box 29: the scattered atom is designated as SE.
22. Box 30: generate random number and determine the probability of inelastic scattering.
23. Box 31: test to determine the type of scattering; if elastic, go to Box 34, otherwise go to Box 32.
24. Box 32: generate random and play for the scattering direction and calculate new wavelength.
25. Box 33: test new wavelength to determine if it can further excite the elements presents; if not, path ended, go to Box 8 and generate new primary photon; otherwise go to Box 12.
26. Box 34: for elastic scattering, determine the direction of scattering, then go to Box 14.
27. Box 35: determine the primary and secondary absorption effects, and activate or update absorption counters.
28. Box 36: test to determine if the absorbed photon can excite the analyte line. If the wavelength is greater than the analyte-line absorption edge, but less than the absorption edge for the L-series, go to Box 47; if the wavelength is greater than the

particular line absorption edge, path is ended, go to Box 8;
otherwise, continue.

29. Box 37: excitation counter is updated.
30. Box 38: generate random number and determine probability of K-emission.
31. Box 39: test for K-emission. If random probability is greater than the K-emission probability, $\omega_K(r_K - 1)/r_K$, then Auger emission will occur, path is ended, go to Box 8; if not, continue.
32. Box 40: generate random number and determine probability of K-alpha emission.
33. Box 41: test for K-alpha emission. If K-beta, go to Box 44; otherwise continue.
34. Box 42: determine enhancement effects and update line emission and enhancement effect counters.
35. Box 43: the wavelength is set equal to the analyte line, K-alpha, go to Box 45.
36. Box 44: the wavelength is set equal to the analyte K-beta.
37. Box 45: generate a random number and play for the emission direction.
38. Box 46: test if the emitted wavelength can excite the elements present; if not, path ended, go to Box 8.
39. Box 47: test if the absorbed photon can excite the L-line of the analyte; if not, path ended, go to Box 8.
40. Box 48: increase the L-excitation counter.

41. Box 49: generate random number and determine the probability of L-emission.
42. Box 50: test for L-emission; if no emission, go to Box 8.
43. Box 51: generate random number and determine the probability of L-alpha emission.
44. Box 52: test for L-alpha emission; if no emission, go to Box 55.
45. Box 53: determine enhancement effects. Increase or update line-emission counter.
46. Box 54: set wavelength equal to the analyte L-alpha, then go to Box 45.
47. Box 55: set wavelength equal to analyte L-averaged line, then go to Box 45.
48. Box 56: determine the relative intensities and/or the inter-element effects.
49. Box 57: print results. If program is completed, exit through Box 2 to STOP.

3.3 The Influence Coefficients

The inter-element effects or influence coefficients are determined by means of a multiple regression analysis of the Monte Carlo simulation intensity data. The regression equation to be used for this analysis is the following,

$$C_i = R_i \sum_{j=1}^n a_{ij} C_j, \quad (3.45)$$

where a_{ij} is the influence coefficient of element j on the line intensity of element i , C is concentration (weight fraction), and R_i is an intensity ratio of the analyte intensity in the sample to the analyte intensity in a reference standard.

The R_i 's, relative intensities of the elements to be analyzed, are obtained as follows. Simulation runs for a sample of 100% A, and multi-element samples containing analyte A, are performed under the same excitation conditions. The number of photons not absorbed by the matrix and emitted by the analyte emerging from the sample is recorded for each different sample. Since the probability of detection is a constant for a given instrument, then the ratio of the analyte-line photons emerging from the multi-element sample to that of the pure sample will correspond to the relative intensity of analyte A.

$$R_i = \frac{(\text{No. of photons emerging})_M \times (\text{Prob. of detection})}{(\text{No. of photons emerging})_P \times (\text{Prob. of detection})} \quad (3.46)$$

where M represents the multi-element sample, and P the pure element sample.

Once the relative intensities of the elements to be analyzed are obtained from the Monte Carlo simulation, the influence coefficients, a_{ij} 's, are found from a regression analysis performed by means of a statistical subroutine MRA (Multiple Regression Analysis), available at the University of Arizona Computer Center. Once the influence coefficients are evaluated, Equation (3.45) can be used to calculate analyte concentrations from measured intensities from samples of similar

compositions as those simulated. See Appendix B for actual listings of the program used for the regression analysis.

3.4 Validation of the Monte Carlo Model

Experimental data from a series of metal standards were used to validate the results thus obtained.

CHAPTER 4

SIMULATION RESULTS

The assessment of the accuracy of the Monte Carlo model was made by comparison with the experimental data of Rasberry and Heinrich (1974). The mass-absorption data of Leraux (1962), Heinrich (1966), and the International Tables of X-Ray Crystallography (1962), and the fluorescent yield data of Colby (1968), and Bambinek et al. (1972) were used throughout the course of this investigation (Table 4.1).

The Ni-Cr-Fe ternary alloy system, in which the inter-element effects are severe, was simulated over the compositional range of 0 to 100% of each element, under the following simulated instrument conditions:

X-ray tube voltage: 45 kV FWR

Angle of incidence: 60°

Take-off angle: 30°

For the same instrument geometry, 60°/30°, simulations were also performed using an applied voltage of 45 kV CP, where CP means constant potential and FWR means full-wave rectified.

Simulations were also performed to study the effect of the number of photons (or trajectories) considered on the relative intensity (Fig. 4.1). A sensitivity test of the Monte Carlo model was performed using various values of the mass-absorption coefficients, while holding

Table 4.1 X-Ray Data. -- k implies the wavelength region to the short side of the absorption edge; k1 implies the wavelength region to the long side of the absorption edge.

		Ni	Fe	Cr
<u>Mass Absorption Coefficients</u>				
Leraux (1962), $\mu = C\lambda^N$	C_k :	118.1	97.61	79.41
	n_k :	2.83	2.83	2.83
	C_{k1} :	15.53	12.54	9.94
	n_{k1} :	2.66	2.66	2.66
Heinrich (1966), $\mu = C\lambda^N$	C_k :	115.9	95.8	78.0
	n_k :	2.71	2.72	2.73
	C_{k1} :	14.8	11.75	9.18
	n_{k1} :	2.73	2.73	2.73
<u>Int'l. Tables of X-Ray Crystallography (1962)</u> $\mu = A\lambda^3 - B\lambda^4 + C$	AA_k :	158.0	126.0	99.0
	B_k :	40.1	27.2	18.2
	A_{k1} :	13.9	9.95	7.24
	B_{k1} :	0.615	0.433	0.268
	C :	0.186	0.183	0.182
<u>Fluorescent Yield</u>				
Colby (1968)		0.392	0.324	0.258
Bambinek et al. (1972)		0.414	0.347	0.282

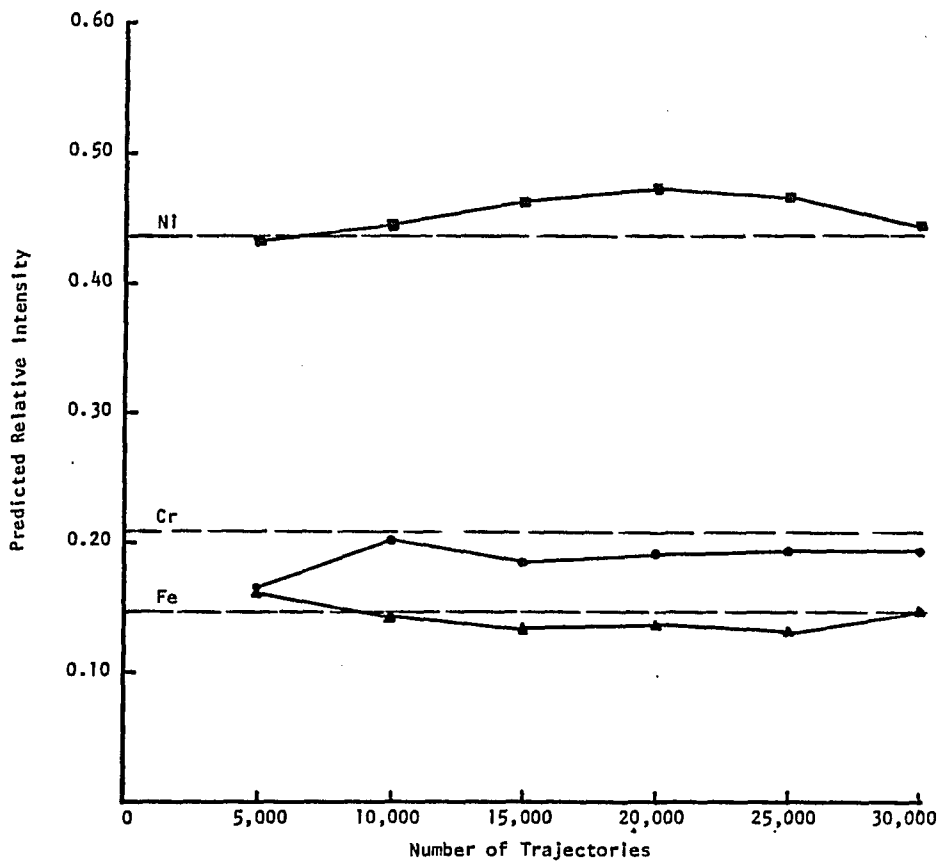


Fig. 4.1 Effect of the Number of Trajectories on the Predicted Relative Intensity.

the fluorescent yield constant, and vice versa. The results are given in Tables 4.2 and 4.3.

In Table 4.4, the relative intensities and their corresponding relative errors are given for several samples of analytical composition similar to the samples used by Rasberry and Heinrich (1974). All the relative intensities were calculated using Equation (3.46) and the data obtained from the Monte Carlo simulations.

The inter-element effects of influence coefficients (Table 4.5) were calculated using the relative intensities given in Table 4.4. Four of the samples were not used in the calibration process, rather they were reserved to be measured and computed as unknowns.

In Table 4.6, analytical results are given for the four samples that were reserved for this purpose. The Monte Carlo results are based on the relative intensities of Table 4.4, while the experimental results are based on the measured intensity data of Rasberry and Heinrich (1974). The analytical results were obtained according to Section 3.3. The relative errors are given in Table 4.7.

Table 4.2 The Effect of the Mass Absorption Coefficient on the Relative Intensity. -- Mass absorption data: IT from International Tables for X-ray Crystallography, L from Leraux (1962), H from Heinrich (1966); fluorescent yield data: Bk from Bambinek et al. (1972).

Weight Fraction				Relative Intensity		
Ni	Cr	Fe		Ni	Cr	Fe
0.2357	0.2784	0.3179	Experimental	0.1115	0.3361	0.3179
			IT-Bk	0.1333	0.3086	0.3066
			L-Bk	0.1232	0.3342	0.3210
			H-Bk	0.1280	0.3145	0.3193
0.6429	0.1688	0.1501	Experimental	0.4367	0.2072	0.1501
			IT-Bk	0.4383	0.2025	0.1395
			L-Bk	0.4202	0.2092	0.1594
			H-Bk	0.4472	0.2020	0.1441
0.3599	--	0.6319	Experimental	0.1720	--	0.6958
			IT-Bk	0.1778	--	0.6748
			L-Bk	0.1677	--	0.6594
			H-Bk	0.1737	--	0.6485
0.8041	0.1897	--	Experimental	0.6556	0.2240	--
			IT-Bk	0.6465	0.2240	--
			L-Bk	0.6388	0.2000	--
			H-Bk	0.6424	0.2117	--

Table 4.3 The Effect of the Fluorescent Yield on the Relative Intensity. -- Mass absorption data: H from Heinrich (1966); fluorescent yield data: C from Colby (1968), and Bk from Bambinek et al. (1972).

Weight Fraction				Relative Intensity		
Ni	Cr	Fe		Ni	Cr	Fe
0.2357	0.2784	0.4721	Experimental	0.1115	0.3361	0.3179
			H-Bk	0.1280	0.3145	0.3193
			H-C	0.1221	0.3435	0.3213
0.7265	0.1540	0.0660	Experimental	0.5534	0.1740	0.0667
			H-Bk	0.5630	0.1867	0.0621
			H-C	0.5558	0.1911	0.0628
0.6429	0.1688	0.1501	Experimental	0.4367	0.2072	0.1460
			H-Bk	0.4472	0.2020	0.1441
			H-C	0.4379	0.2133	0.1445
0.6064	0.3883	--	Experimental	0.4111	0.4305	--
			H-Bk	0.4222	0.4031	--
			H-C	0.4042	0.4127	--
0.8041	0.1897	--	Experimental	0.6556	0.2240	--
			H-Bk	0.6424	0.2117	--
			H-C	0.6442	0.2355	--
0.3599	--	0.6315	Experimental	0.1720	--	0.6958
			H-Bk	0.1737	--	0.6485
			H-C	0.1726	--	0.6860

Table 4.4 Predicted Relative Intensities. -- Based on the mass absorption data of Heinrich (1966) and the fluorescent yield data of Bambinek et al. (1972).

Weight Fraction				Relative Intensity		
Ni	Cr	Fe		Ni	Cr	Fe
0.6428	0.1688	0.1501	Experimental	0.4367	0.2072	0.1460
				0.4472 (+2.39)	0.2020 (-2.41)	0.1441 (+1.3)
0.1927	0.2696	0.5280	Experimental	0.0810	0.3311	0.3529
				0.1016 (+23.0)	0.3249 (-1.9)	0.3523 (-.85)
0.7265	0.1540	0.066	Experimental	0.5534	0.1740	0.0667
				0.5630 (+1.7)	0.1867 (+7.3)	0.0621 (-6.8)
0.2357	0.2784	0.4721	Experimental	0.1115	0.3361	0.3179
				0.1280 (+14.9)	0.3145 (-6.4)	0.3193 (+.44)
0.0996	0.1988	0.6945	Experimental	0.0416	0.2651	0.4971
				0.0407 (-2.2)	0.2634 (-0.6)	0.4968 (-0.1)
0.1927	0.2696	0.5280	Experimental	0.0821	0.3311	0.3529
				0.0774 (-5.72)	0.3171 (-4.83)	0.3769 (+6.8)
0.6064	0.3883	--	Experimental	0.4111	0.4305	--
				0.4222 (+2.7)	0.4031 (-6.4)	--
0.8041	0.1897	--	Experimental	0.6556	0.2240	--
				0.6424 (-2.0)	0.2117 (-5.5)	--
0.7343	0.2621	--	Experimental	0.5543	0.2873	--
				0.5711 (+3.0)	0.2632 (+8.4)	--
0.7858	0.2096	--	Experimental	0.6515	0.2304	--
				0.6517 (+0.03)	0.2174 (-5.6)	--

Table 4.4, Continued.

Weight Fraction				Relative Intensity		
Ni	Cr	Fe		Ni	Cr	Fe
0.7192	0.3360	--	Experimental	0.5392 0.5560 (+3.1)	0.3174 0.2789 (-8.9)	-- -- --
--	0.0608	0.9372	Experimental	-- -- --	0.1004 0.1154 (+14.9)	0.8270 0.7605 (-8.0)
--	0.3658	0.6322	Experimental	-- -- --	0.4476 0.4348 (-2.9)	0.3579 0.3457 (-3.4)
--	0.2503	0.7747	Experimental	-- -- --	0.3326 0.3529 (+6.1)	0.4748 0.4945 (+4.1)
0.6520	--	0.3431	Experimental	0.4073 0.3984 (-2.2)	-- -- --	0.4373 0.4479 (+2.5)
0.3599	--	0.6315	Experimental	0.1720 0.1737 (+0.99)	-- -- --	0.6958 0.6485 (+6.8)
0.4820	--	0.510	Experimental	0.2553 0.2622 (+2.7)	-- -- --	0.5907 0.5543 (-6.2)

Table 4.5 Inter-Element Coefficients for the Ternary System Ni-Cr-Fe. -- The coefficients were based on the data obtained from the Monte Carlo simulation using the mass-absorption data of Heinrich (1966) and the fluorescent yield data of Bambinek et al. (1972).

X-Ray Line	Ni	Cr	Fe
Ni Ka	1.01646	2.16111	2.72463
Cr Ka	0.84524	1.14946	0.62223
Fe Ka	0.61702	3.12365	1.03952

Table 4.6 Calculated Concentrations (Weight Fractions). -- The analytical values were determined by wet chemical analysis, as reported by Rasberry and Heinrich (1974). The experimental values were obtained by a regression analysis of the measured intensity reported by Rasberry and Heinrich (1974).

Sample	Method	Ni	Cr	Fe
1	Analytical	0.6552	0.0000	0.3431
	Monte Carlo	0.6579	0.0000	0.3420
	Experimental	0.6622	0.0000	0.3378
2	Analytical	0.0015	0.2577	0.7250
	Monte Carlo	0.0015	0.2531	0.7453
	Experimental	0.0016	0.2594	0.7390
3	Analytical	0.1480	0.2130	0.6303
	Monte Carlo	0.1507	0.2140	0.6354
	Experimental	0.1547	0.2181	0.6273
4	Analytical	0.7265	0.1540	0.0660
	Monte Carlo	0.7509	0.1513	0.0979
	Experimental	0.7538	0.1474	0.0987

Table 4.7 Calculated Relative Errors (%). -- Experimental values are based on Rasberry and Heinrich's (1974) measured intensity data.

Sample	Method	Ni	Cr	Fe
1	Monte Carlo	+0.41	0.00	-0.32
	Experimental	+1.07	0.00	-1.54
2	Monte Carlo	0.00	-1.79	+2.73
	Experimental	+6.67	+0.66	+1.93
3	Monte Carlo	+1.82	+0.47	+0.81
	Experimental	+4.53	+2.39	-0.48
4	Monte Carlo	+3.36	-1.75	+48.33
	Experimental	+3.76	+4.29	+49.54

CHAPTER 5

DISCUSSION OF RESULTS

There are three main sources of error in a simulation of this type. The first is statistical, the result of the finite number of trajectories or primary photons considered. The second is systematic, introduced by the spectral distribution of the energy source used; and the third is from the inaccuracies of the x-ray data used.

5.1 The Statistical Error

The statistical error can be reduced by increasing the number of primary photons used, the accuracy of any parameter increasing as the square of the number of photons considered. Since the whole simulation process has a statistical basis, the estimate of the relative error is

$$\text{Error (\%)} = \pm 100 \times \sqrt{9(1 - R_i)/R_i N} , \quad (5.1)$$

where N is the number of photons considered, and R_i is the calculated relative intensity. From Equation (5.1), if the statistical error is to be reduced by one order of magnitude, the number of photons must be increased by a factor of 100. But there is no point in reducing the statistical error below those arising from other sources.

The effect of the number of photons on the relative intensity is illustrated in Fig. 4.1, and the relative intensities and their corresponding relative error are given in Table 5.1. All other simulations

Table 5.1 Effect of the Number of Photons on the Relative Intensity.

	<u>Ni</u>	<u>Cr</u>	<u>Fe</u>
Sample weight fraction:	0.6429	0.1688	0.1501
Relative intensity:	0.4367	0.2072	0.1460

Number of Photons	Relative Intensity		
	Ni	Cr	Fe
5,000	0.4309 (-1.33)	0.1634 (-21.14)	0.1614 (+10.54)
10,000	0.4472 (+2.39)	0.2020 (-2.41)	0.1441 (+1.31)
15,000	0.4631 (+6.04)	0.1868 (-9.85)	0.1386 (-5.07)
20,000	0.4708 (+7.81)	0.191 (-7.82)	0.1398 (-4.25)
25,000	0.4695 (+7.51)	0.1966 (-5.12)	0.1343 (-8.01)
30,000	0.4485 (+2.27)	0.1968 (-5.02)	0.1464 (+0.21)

were based on 10,000 photons, since the relative error did not change considerably within this range.

5.2 Energy Source

Two x-ray tubes were simulated, one with an applied voltage of 45 KV CP, and the other with an applied voltage of 45 KV FWR. For the FWR applied voltage, there is less intensity in the short-wavelength portion of the continuum. This may or may not be important, depending on the elements to be excited in the sample. In the present investigation, the full-wave rectified applied voltage was used to reduce the line intensity of Ni.

The spectral distribution of an x-ray tube operating at constant potential, CP, is given by,

$$I(\lambda)d\lambda = KiZ \left[\frac{\lambda}{\lambda_{swl}} - \lambda^{-2} \right] d\lambda , \quad (3.21)$$

and for the full-wave rectified potential,

$$I(\lambda)d\lambda = CiZ \frac{1}{\lambda^{-2}\lambda_{swl}} \left[\lambda \cos \sin^{-1} \left(\frac{\lambda_{swl}}{\lambda} \right) - \lambda_{swl} \left[\frac{\pi}{2} - \sin^{-1} \frac{\lambda_{swl}}{\lambda} \right] \right] d\lambda . \quad (5.2)$$

These equations were numerically solved according to Section 3.1.1 to obtain a polynomial equation of the wavelength as a function of random number, as given by,

$$\lambda = 0.3074 + 3.0216r - 10.9973r^2 + 34.1240r^3 - 52.7779r^4 + 40.6418r^5 - 12.2244r^6, \quad (5.3)$$

for the 45 KV FWR, and

$$\lambda = 0.2663 + 2.1367r - 5.8527r^2 + 18.6410r^3 - 27.0634r^4 + 20.8460r^5 - 6.1450r^6 \quad (5.4)$$

for the 45 KV CP. These equations are illustrated in Fig. 5.1.

All the simulations were performed using a simulated applied voltage of 45 KV FWR, since the experimental data used to validate the Monte Carlo model were obtained under similar conditions. Also, the relative intensities calculated with an applied voltage of 45 KV CP were virtually the same as for the 45 KV FWR potential.

Accurate description of the spectral distribution of the x-ray tube or energy source is required, since it governs both the frequency and energy of the exciting primary x-ray beam for the energy or wavelength range to be simulated. Furthermore, the energy source to be used in the simulation model should be the same as the one in the spectrometer to be used in order to reduce the error introduced by the spectral distribution. A relative error less than 2% is introduced during the least-squares fit of the wavelength and the random number data, that contributes to the total error of the Monte Carlo model.

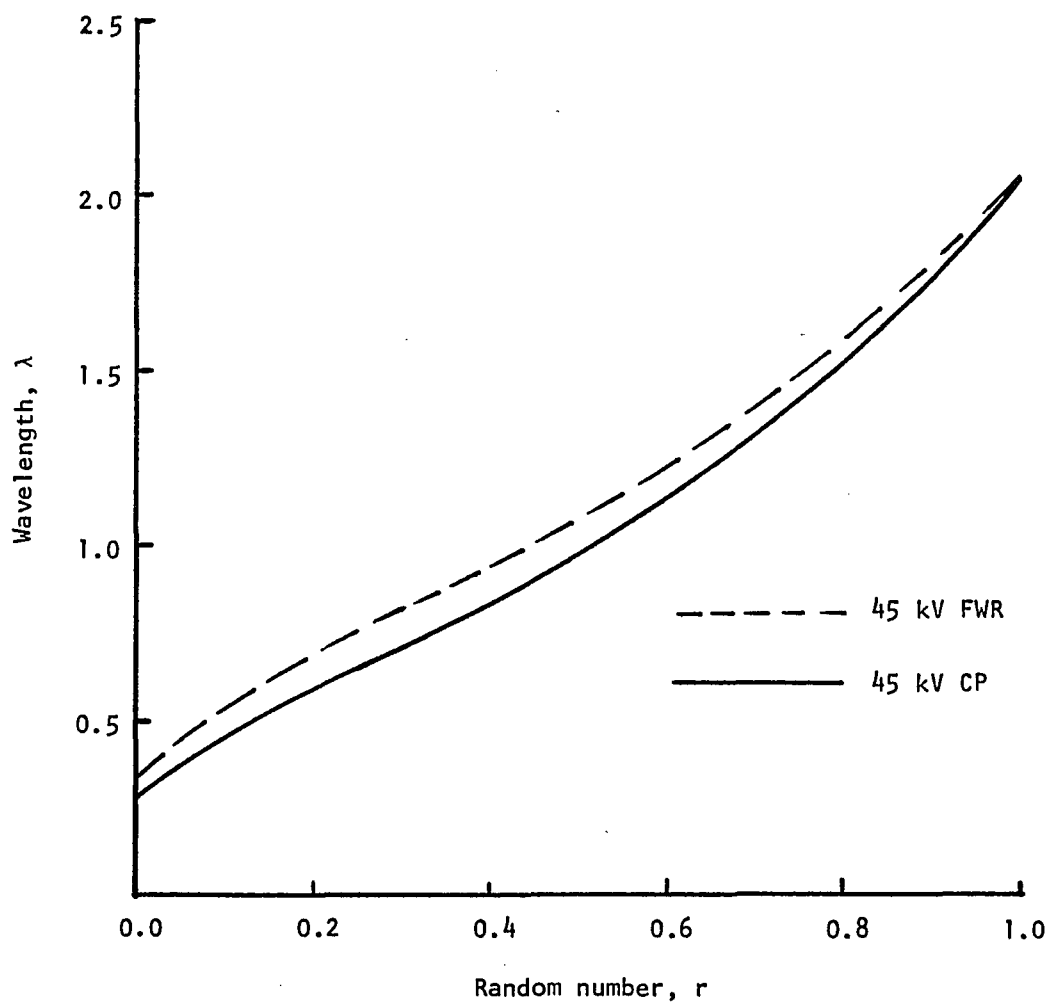


Fig. 5.1 Comparison between the 45 kV CP and 45 kV FWR Random Wavelength Distribution.

5.3 Inaccuracy of the X-Ray Data

The inaccuracies of the x-ray data also contribute to the total error of the Monte Carlo method. Simulations were performed to determine the sensitivity of the Monte Carlo model to changes in the mass-absorption coefficients and fluorescent yields; the results are given in Tables 4.2 and 4.3. When the fluorescent yield was held constant and the mass-absorption coefficients were varied, a relative error of 3% was calculated. For the simulation in which the mass-absorption coefficient was held constant and the fluorescent yields were varied, a relative error of 4% was calculated.

The shortcoming of the uncertainties in the x-ray data available, such as the mass-absorption coefficient and fluorescent yield, is being overcome rapidly, since many investigators are devoting themselves to remeasuring the required data.

5.4 Analytical Results

Influence coefficients were calculated from the relative intensities obtained from the Monte Carlo simulations; results are given in Table 4.5. Similar coefficients were also calculated using the measured intensity data of Rasberry and Heinrich (1974) (Table 5.2). These influence coefficients were then applied in accordance with Section 3.3 to the relative intensities of the four samples that were reserved to be analyzed as unknowns. The analytical results are given in Table 4.6 and the relative errors in Table 4.7.

The results show good agreement with the analytical values obtained by wet chemical analysis, as reported by Rasberry and Heinrich

Table 5.2 Inter-Element Coefficients for the Ternary System Ni-Cr-Fe. -- The coefficients were based on the experimental data reported by Rasberry and Heinrich (1974).

X-Ray Line	Ni	Cr	Fe
Ni Ka	0.99828	2.25181	2.81238
Cr Ka	0.83373	1.02457	0.68689
Fe Ka	0.68829	2.45114	1.06486

(1974). The average relative error was less than 1% for all but 1 of 12 values. The high relative error obtained for Fe in sample 4 leads to the belief that the regression model used to calculate the analytical compositions does not apply to samples containing low concentration of Fe. The same result was obtained for both data used. No other explanation was found for such behavior.

The results given in Chapter 4 indicate that the Monte Carlo simulation model is a practical method to obtain the relative intensity data required for calibration methods without the use of calibration standards.

CHAPTER 6

SUMMARY AND CONCLUSIONS

A Monte Carlo method has been developed to simulate the x-ray fluorescence process within a homogeneous multi-element mixture. The model was successfully applied to a Ni-Cr-Fe system in which the inter-element effects are severe.

Relative intensities for each sample analyzed were obtained by means of the Monte Carlo simulation. The associated error of the predicted relative intensities was less than 10%, which is probably as accurately as the model parameters (mass absorption coefficients and fluorescent yields) are known.

The results indicate that the Monte Carlo model that has been developed is a practical simulator for the x-ray fluorescence from a homogeneous multi-element mixture and may be used in place of standards to obtain the intensity data required, when good mass absorption and fluorescent yield data are available.

CHAPTER 7

SUGGESTIONS FOR FUTURE WORK

The success of the Monte Carlo model indicates that it could be applied to more complex systems. Although it proved to be useful for systems in which the K_{α} line was the spectral line to be measured, the model should be expanded and tested to include systems involving the emission of the L_{α} and other lines of interest.

The spectral distribution of the x-ray tube primary beam is of great importance in this type of calculation. Therefore, more reliable equations or empirical relations describing the different types of x-ray tubes that are available for x-ray spectrochemical analysis should be developed to improve the accuracy of the model. Also, further study is required to reduce the uncertainty of the x-ray data available.

APPENDIX A

X-RAYS, A FORTRAN IV PROGRAM FOR THE MONTE CARLO
SIMULATION OF THE X-RAY FLUORESCENCE PROCESS

PROGRAM XRAYS

73/74 OPT=0 TRACE

FTN 4.6+428

```

1      PROGRAM XRAYS (INPUT,OUTPUT,TAPES = INPUT,TAPE6 = OUTPUT)
C.....
C      A MONTE CARLO ANALYSIS OF THE INTERELEMENT EFFECTS IN
C      X-RAY FLUORESCENCE ANALYSIS. THIS IS ACHIEVED BY
5      SIMULATING THE PROCESS OF X-RAYS SECONDARY EMISSION
C      OR FLUORESCENCE IN A HOMOGENEOUS MATRIX OF KNOWN
C      COMPOSITION. PHOTONS OF RANDOM ENERGY OR WAVELENGTH
C      ARE GENERATED AND THEIR PATHS THROUGH THE SPECIMEN
C      ARE STUDIED BY ANALYZING ALL THE EVENTS THAT ARE
10     INVOLVED IN THE PROCESS. THE INTENSITY DATA OBTAINED
C      WILL BE USED TO DETERMINE THE INFLUENCE COEFFICIENTS.
C.....
C      REAL NK(10),NKL(10),K1(10),K2(10),KA(10),KAA(10,10),
15     1K2A(10),KA1(10),KA2(10),K1AJ(10,10),K2AJ(10,10),L1(10),
2LA(10),LAA(10,10),L1AJ(10,10),L2AJ(10,10),L2(10),L3(10),
3LA1(10),LA2(10),KAE(10,10,10),LAE(10,10,10),K3(10),
4LA3(10),K3AJ(10,10),L3AJ(10,10),KAS(10,10),LAS(10,10),
5KA3(10),LAES(10,10),KTP(10),KAES(10,10,10),K3A(10),
6KEX1(10),KEX2(10,10),KEX3(10,10),KEM1(10),KEM2(10,10),
20     7K1A(10),L1A(10),L2A(10),LTP(10),KEM3(10,10),L3A(10),
8KEP(10),LEP(10)
C
C      INTEGER Z,X,D
C
25     DIMENSION Z(10),AW(10),XK(10),XKA(10),XKB(10),XL1(10),
1XL3(10),XLA(10),XLM(10),CK(10),CKL(10),CL1(10),CL2(10),
2TOA(10),W(10),WL(10),RHO(10),ELEM(10),RK(10),RL(10),
3GL(10),EMAC(10),EMSC(10),XKW(10),XLW(10),ATPER(10),
4SUM(10),PI(10),SI(10),TI(10),PAC(10),PSI(10),PTI(10),
30     5NEE(10),TP(10),B1(10,10),MXA(10),PSUM(10,10),SKAA(10),
6SL1AJ(10),SK1AJ(10),SLAA(10),RC(10),PSCAT(10),Y(10),
7XL2(10),CLM(10),C(10),RI(10)
8,A1(3),A2(3),A3(3),A4(3),A5(3)
C.....
C      READ PROGRAM PARAMETERS AND X-RAY DATA
C.....
40     READ (5,1) NE,NR,LAI,IOR,NPP
      READ (5,183) GK,NLM,AOI,EMX
      READ (5,2) (Z(J),J=1,NE), (AW(J),J=1,NE), (RHO(J),J=1,NE),
1(XK(J),J=1,NE), (XKA(J),J=1,NE), (XKB(J),J=1,NE), (W(J),
2J=1,NE), (ELEM(J),J=1,NE), (CK(J),J=1,NE), (CKL(J),J=1,
3NE), (NK(J),J=1,NE), (NKL(J),J=1,NE), (TOA(J),J=1,NE)
      READ (5,182) (RC(I),I=1,IOR)
45     READ (5,181) (TI(J),J=1,NE)
      READ (5,90) VOLT,GEO
C.....
C      PHI = ANLGE OF INCEDENCE WRT THE SURFACE NORMAL
C.....
50     PHI=(90.-AOI)/57.2957795
      AOI=AOI/57.2957795
      IF (NE.LT.LAI) GO TO 8
C.....
C      IF THE L-ALPHA LINE IS TO BE TESTED, READ L-DATA
C.....
55     READ (5,5) (XL1(J),J=1,NE), (XL2(J),J=1,NE), (XL3(J),
1J=1,NE), (XLA(J),J=1,NE), (XLM(J),J=1,NE), (CL1(J),J=1,NE),
2(CL2(J),J=1,NE), (CLM(J),J=1,NE), (WL(J),J=1,NE),

```

PROGRAM XRAY5

73/74 OPT=0 TRACE

FTN 4.6+428

```

      3(GL(J),J=1,NE)
C.....
60  C.....
C     PRELIMINARY CALCULATIONS TO DETERMINE THE ABSORPTION
C     EDGE JUMP RATIOS, ATOMIC PERCENTS, MATRIX DENSITY
C     AND EMISSION COEFFICIENTS.
C.....
65  8 DO 160 LI=1,NR
      READ (5,7) (C(J),J=1,NE)
      DENS=0.
      SIGMA=0.
      DO 10 I=1,NE
70  DENS=DENS +C(I)*RHO(I)
      10 SIGMA=SIGMA+C(I)/AW(I)
      DO 11 I=1,NE
      ATPER(I)=(C(I)/AW(I))/SIGMA
      RK(I)=(CK(I)/CKL(I))*XK(I)**(NK(I)-NKL(I))
75  XKW(I)=W(I)*(1.-1./RK(I))
      IF (I.GE.LAI) RL(I)=CKL(I)/CLM(I)
      11 CONTINUE
C.....
C     PRINT DATA
80  C.....
      WRITE (6,3) NPP,(ELEM(J),J=1,NE)
      WRITE (6,4) (C(J),J=1,NE)
      WRITE (6,149) (RHO(J),J=1,NE)
      WRITE (6,150) (CK(J),J=1,NE)
85  WRITE (6,151) (CKL(J),J=1,NE)
      WRITE (6,152) (NK(J),J=1,NE)
      WRITE (6,153) (NKL(J),J=1,NE)
      WRITE (6,100) (ATPER(J),J=1,NE)
      WRITE (6,180) (AW(J),J=1,NE)
90  WRITE (6,142) (XK(J),J=1,NE)
      WRITE (6,143) (XKA(J),J=1,NE)
      WRITE (6,144) (RK(J),J=1,NE)
      WRITE (6,147) (W(J),J=1,NE)
      IF (NE.LT.LAI) GO TO 48
95  WRITE (6,131) (XL3(J),J=1,NE)
      WRITE (6,132) (XLA(J),J=1,NE)
      WRITE (6,133) (RL(J),J=1,NE)
      WRITE (6,134) (WL(J),J=1,NE)
      48 WRITE (6,91) VOLT,GEO
100 WRITE (6,120) DENS
      CALL RANSET(112869)
C.....
C     INITIALIZE COUNTERS
C.....
105 MAX=0
      DO 12 N=1,NE
      KA(N)=0
      KA1(N)=0.
      KA2(N)=0
110 K1(N)=0
      K2(N)=0
      K1A(N)=0
      K2A(N)=0
      KEP(N)=0.

```

PROGRAM XRAYS

73/74 OPT=0 TRACE

FTN 4.6+428

```

115      KTP(N)=0.
          PI(N)=0.
          SI(N)=0.
          BI(N)=0.
          DO 12 L=1,NE
120      B1(N,L)=0.
          KAA(N,L)=0
          K1AJ(N,L)=0
          K2AJ(N,L)=0
          12 CONTINUE
125      C.....
          C
          C      START THE MONTE CARLO ANALYSIS
          C
          C      GENERATE RANDOM NUMBER AND CALCULATE RANDOM WAVELENGTH
130      C.....
          KP=0
          DO 25 LL=1,NPP
          RN=RANF(0.)
          C.....
135      C      THE RANDOM WAVELENGTH IS GIVEN BY A POLYNOMIAL
          C      OF THE FORM,
          C      RAWAVE= A + B*RN + C*RN**2 + D*RN**3 +...
          C.....
          RAWAVE=0.
140      DO 13 I=1,IOR
          II=I-1
          IF (I.EQ.1) RAWAVE=RAWAVE+RC(I)
          IF (I.NE.1) RAWAVE=RAWAVE+RC(I)*RN**II
          13 CONTINUE
145      DO 41 J=1,NE
          IF (RAWAVE.LE.XK(J).AND.C(J).NE.0.) K1(J)=K1(J)+1
          41 CONTINUE
          C.....
150      C      AUXILIARY COMPUTATIONS
          C.....
          KP=KP+1
          D=1
          M=0
          NA=0
          K=0
155      DO 42 I=1,10
          42 Y(I)=0.
          14 XMAC=0.
          XLAC=0.
160      V=0.024264/RAWAVE
          TA=1.+2*V
          Q=RAWAVE**3.
          C.....
          C      DETERMINE MASS ABSORPTION AND SCATTERING COEFFICIENTS
165      C.....
          DO 27 J=1,NE
          IF (RAWAVE.LE.XK(J)) EMAC(J)=CK(J)*RAWAVE**NK(J)
          IF (RAWAVE.GT.XK(J)) EMAC(J)=CKL(J)*RAWAVE**NKL(J)
          PAC(J)=0.
          PSCAT(J)=0.
170      XMAC=XMAC+EMAC(J)*C(J)

```

PROGRAM XRAY5

73/74 OPT=0 TRACE

FTN 4.6+428

```

27 XLAC=XLAC+EMAC (J) *C (J) *RHO (J)
C.....
C CALCULATE THE CORRESPONDING PROBABILITIES OF
175 C ABSORPTION AND SCATTERING
C
      DO 15 J=1,NE
      EMSC (J) = (0.4005/TA) *Z (J) /AW (J)
      PAC (J) =EMAC (J) *C (J) *RHO (J) /XLAC
180      15 PSCAT (J) =C (J) *EMSC (J) /XMAC
      PCSCAT=B/TA
C
C.....
C DETERMINE THE RANDOM DISTANCE TRAVELLED WITHOUT
185 C COLLISION AND THE PENETRATION
C.....
      9 K=K+1
      23 RN=RANF (0.)
      IF (RN.EQ.0.) GO TO 23
      FP=-ALOG (RN) /XLAC
      IF (FP.EQ.0..AND.D.EQ.1) GO TO 24
      IF (FP.EQ.0..AND.D.EQ.2) GO TO 18
190      24 IF (D.EQ.1) Y (K) =FP *COS (PHI)
      IF (D.NE.1) Y (K) =Y (K-1) +FP *COSA
195      IF (Y (K) .LT.0) GO TO 46
C.....
C GENERATE RANDOM PROBABILITY OF COLLISION AND
C DETERMINE THE ATOM THAT WILL COLLIDE WITH THE PHOTON
200 C.....
      COLPRO=RANF (0.)
      NEP1=NE+1
      DO 44 I=1,NEP1
      44 SUM (I) =0.
      DO 16 J=1,NE
205      SUM (J+1) =SUM (J) +PAC (J)
      IF (COLPRO.GT.SUM (J) .AND.COLPRO.LE.SUM (J+1)) GO TO 17
      16 CONTINUE
C.....
C X REPRESENTS THE COLLIDING ATOM
210 C.....
      17 X=J
      IF (D.EQ.1) E=1.
      IF (D.EQ.2) E=2.
C.....
215 C GENERATE RANDOM PROBABILITY OF SCATTERING AND
C DETERMINE IF PHOTON WILL BE ABSORBED OR SCATTERED
C.....
      COLTYP=RANF (0.)
      IF (COLTYP.GT.PSCAT (X)) GO TO 18
220 C.....
C PHOTON WAS SCATTERED.
C DETERMINE THE RANDOM ANGLE OF SCATTERING AND
C THE TYPE OF SCATTERING
C.....
225 C COMPTON SCATTERING.....SE REPRESENTS SCATTERING ELEMENT
C.....
      SE=X
      D=3

```

PROGRAM XRAYS

73/74 OPT=0 TRACE

FTN 4.6+428

```

SCATTP=RANF(0.)
230 IF (SCATTP.GT.PCSCAT) GO TO 19
RN=RANF(0.)
S=V/(1.+0.5625*V)
AC=V/(1.+S*RN+(2.-S)*RN**3)
RAWAVE=0.024264/AC
235 COSA=1.+(1./V)-(1./AC)
IF (RAWAVE.GT.EMX) GO TO 25
GO TO 14

C.....
C ELASTIC SCATTERING
240 C.....
19 RN=RANF(0.)
COSA=1.-2.*RN
GO TO 9

C.....
245 C PHOTON WAS ABSORBED.
C GENERATE RANDOM PROBABILITY OF EMISSION AND
C DETERMINE TYPE OF EMISSION...K OR AUGER
C.....
250 18 IF (D.EQ.1) K1A(X)=K1A(X)+1
IF (D.EQ.2) K2A(X)=K2A(X)+1
C.....
C DETERMINE PRIMARY AND SECONDARY ABSORTION EFFECTS
C
DO 29 I=1,NE
255 IF (RAWAVE.EQ.XKA(I).AND.D.EQ.2) KAA(I,X)=KAA(I,X)+1
IF (RAWAVE.LE.XK(I).AND.D.EQ.1.AND.C(I).NE.0.)
1K1AJ(I,X)=K1AJ(I,X)+1
IF (RAWAVE.LE.XK(I).AND.D.EQ.3.AND.E.EQ.1.AND.C(I).NE.0)
260 1K1AJ(I,X)=K1AJ(I,X)+1
IF (RAWAVE.LE.XK(I).AND.D.EQ.2.AND.C(I).NE.0.)
1K2AJ(I,X)=K2AJ(I,X)+1
IF (RAWAVE.LE.XK(I).AND.D.EQ.3.AND.E.EQ.2.AND.C(I).NE.0)
1K2AJ(I,X)=K2AJ(I,X)+1
29 CONTINUE
265 C.....
C
C.....
C TEST IF PHOTON WILL EXCITE THE K-SERIES
270 IF (RAWAVE.GT.XK(X).AND.X.LT.LAI) GO TO 25
C.....
C.....
C DETERMINE TYPE OF EMISSION.....K OR AUGER
C.....
275 PROKE=RANF(0.)
IF (PROKE.GT.XKW(X)) GO TO 25
C.....
C GENERATE RANDOM PROBABILITY OF EMISSION AND
C DETERMINE TYPE OF EMISSION.. K-ALPHA OR K-BETA
C.....
280 PROKA=RANF(0.)
IF (PROKA.GT.GK) GO TO 35
20 RAWAVE=XKA(X)
KA(X)=KA(X)+1
285 IF (D.EQ.1) KA1(X)=KA1(X)+1
IF (D.EQ.2) KA2(X)=KA2(X)+1

```

PROGRAM XRAYS 73/74 OPT=0 TRACE

FTN 4.6+428

```

      IF (D.EQ.3.AND.E.EQ.1) KA1(X)=KA1(X)+1
      IF (D.EQ.3.AND.E.EQ.2) KA2(X)=KA2(X)+1
      GO TO 80
290   35 RAWAVE=XKB(X)
      80 RN=RANF(0.)
      COSA=1.-2.*RN
      DO 28 L=1,NE
      IF (RAWAVE.LE.XK(L).AND.C(L).NE.0.) K2(L)=K2(L)+1
295   28 CONTINUE
      D=2
      C.....
      C      M REPRESENTS THE ENHANCING ELEMENT
      C
      M=X
300   C.....
      C      TEST IF NEW WAVELENGTH IS SMALLER THAN THE
      C      MAXIMUM K-ABSORPTION EDGE
      C.....
305   21 IF (RAWAVE.LE.EMX) GO TO 14
      GO TO 25
      C.....
      C      TOTAL NUMBER PHOTONS EMERGING FROM SAMPLE
      C.....
310   46 DO 49 J=1,NE
      49 IF (RAWAVE.EQ.XKA(J)) KEP(J)=KEP(J)+1
      C.....
      C      END OF PHOTON TRAJECTORY
      C      GO BACK AND GENERATE A NEW PHOTON
      C.....
315   25 CONTINUE
      C.....
      C      PRINT RESULTS
      C.....
320   WRITE (6,50)
      WRITE (6,66) (ELEM(J),J=1,NE)
      WRITE (6,51) (K1(J),J=1,NE)
      WRITE (6,64)
      WRITE (6,66) (ELEM(J),J=1,NE)
      WRITE (6,65) (K1A(J),J=1,NE)
325   WRITE (6,54)
      DO 60 J=1,NE
      60 WRITE (6,55) ELEM(J), (K1AJ(J,I),I=1,NE)
      WRITE (6,66) (ELEM(J),J=1,NE)
      WRITE (6,67)
330   WRITE (6,66) (ELEM(J),J=1,NE)
      WRITE (6,68) (K2(J),J=1,NE)
      WRITE (6,74)
      WRITE (6,66) (ELEM(J),J=1,NE)
      WRITE (6,75) (K2A(J),J=1,NE)
335   WRITE (6,52)
      WRITE (6,66) (ELEM(J),J=1,NE)
      WRITE (6,53) (KA(J),J=1,NE)
      WRITE (6,56)
      WRITE (6,66) (ELEM(J),J=1,NE)
340   DO 61 J=1,NE
      61 WRITE (6,57) ELEM(J), (KAA(J,I),I=1,NE)
      WRITE (6,66) (ELEM(J),J=1,NE)

```

PROGRAM XRAYS

73/74 OPT=0 TRACE

FTN 4.6+428

```

      WRITE (6,179)
      WRITE (6,66) (ELEM(J),J=1,NE)
345      WRITE (6,172) (KA1(J),J=1,NE)
      WRITE (6,82)
      WRITE (6,66) (ELEM(J),J=1,NE)
      WRITE (6,83) (KA2(J),J=1,NE)
C.....
C      DETERMINE RELATIVE INTENSITIES
C.....
      DO 30 J=1,NE
      IF (C(J).EQ.1.) TI(J)=KEP(J)
      IF (C(J).EQ.0) GO TO 30
355      IF (TI(J).EQ.0) TI(J)=KA(J)
      PI(J)=(KA1(J)/KA(J))*KEP(J)/TI(J)
      SI(J)=(KA2(J)/KA(J))*KEP(J)/TI(J)
      RI(J)=PI(J)+SI(J)
360      30 CONTINUE
      WRITE (6,145)
      WRITE (6,66) (ELEM(J),J=1,NE)
      WRITE (6,146) (KEP(J),J=1,NE)
      WRITE (6,173) KP
      WRITE (6,66) (ELEM(J),J=1,NE)
365      WRITE (6,174) (PI(J),J=1,NE)
      WRITE (6,175) (SI(J),J=1,NE)
      WRITE (6,178) (RI(J),J=1,NE)
C.....
C      GO BACK AND READ A NEW SET OF CONCENTRATIOIS
370 C.....
      160 CONTINUE
C.....
C      INPUT AND OUTPUT FORMATS
C.....
375      1 FORMAT (4I3,I6)
      2 FORMAT (3I3/3F7.3/3F6.3/3F7.4/3F7.4/3F7.4/3F7.4/3A2/
      13F8.3/3F8.3/3F4.2/3F4.2/3F5.1)
      3 FORMAT (1H1,35X*X-RAYS FLUORESCENCE ANALYSIS BASED
380      1 ON *I6* PHOTONS*//5X*ELEMENT*20XA2,7(11XA2)//)
      4 FORMAT (5X*CONCENTRATION (W/O)*,8(5XF8.5)//)
      5 FORMAT (5F7.4/5F7.4/5F7.4/5F7.4/5F7.4/5F8.3/5F8.3/
      15F8.3/5F7.4/5F5.3)
      6 FORMAT (5X,I2,1X,A2,4XF12.8,7(3XF12.8)//)
      7 FORMAT (8F6.4)
385      50 FORMAT (//35X*PRIMARY PHOTONS THAT COULD EXCITE J*/)
      51 FORMAT (5X*K1(J) *8(5XF10.0)//)
      52 FORMAT (35X*K-ALPHA PHOTONS EMITTED BY ELEMENT J*/)
      53 FORMAT (5X*KA(J) *8(5XF10.0)//)
      54 FORMAT (35X*PRIMARY PHOTONS THAT COULD EXCITE J
390      1 ABSORBED BY I*/)
      55 FORMAT (5X*K1AJ(*A2*,I)*2XF10.0,7(5XF10.0)//)
      56 FORMAT (//35X*K-ALPHA PHOTONS EMITTED BY J AND
      1 ABSORBED BY I*/)
      57 FORMAT (5X*KAA(*A2*,J)*3XF10.0,7(5XF10.0)//)
395      64 FORMAT (35X*PRIMARY PHOTONS ABSORBED BY J*/)
      65 FORMAT (5X*K1A(J) *8(5XF10.0)//)
      66 FORMAT (/5X*ELEMENT*11XA2,7(13XA2)//)
      67 FORMAT (35X*SECONDARY PHOTONS THAT COULD EXCITE J*/)
      68 FORMAT (5X*K2(J) *8(5XF10.0)//)

```

PROGRAM XRAYS

73/74 OPT=0 TRACE

FTN 4.6+428

```

400      69 FORMAT (35X*SECONDARY PHOTONS THAT COULD EXCITE J
          1 ABSORBED BY I*/)
          71 FORMAT (5X*K2AJ (*A2*, I) *2XF10.0,7 (5XF10.0) /)
          74 FORMAT (//35X*SECONDARY PHOTONS ABSORBED BY J*/)
405      75 FORMAT (5X*K2A (J) *8 (5XF10.0) //)
          82 FORMAT (35X*K-ALPHA EMISSION DUE TO SECONDARY PHOTONS*/)
          83 FORMAT (5X*KA2 (J) *8 (5XF10.0) //)
          90 FORMAT (A10, A7)
          91 FORMAT (5X*APPLIED VOLTAGE *A10, 10X*INSTRUMENT GEOMETRY *
          1A7//)
410      100 FORMAT (5X*ATOMIC PERCENT*5X,8 (5XF8.5) //)
          120 FORMAT (5X*MATRIX DENSITY = *F8.4////)
          131 FORMAT (5X*L-ABSORPTION EDGE*2X,8 (5XF8.5) //)
          132 FORMAT (5X*L-ALPHA*12X,8 (5XF8.5) //)
          133 FORMAT (5X*L-ABSN JUMP RATIO*2X,8 (5XF8.5) //)
415      134 FORMAT (5X*L-FLUORESCENT YIELD*8 (5XF8.5) //)
          142 FORMAT (5X*K-ABSORPTION EDGE*2X,8 (5XF8.5) //)
          143 FORMAT (5X*K-ALPHA*12X,8 (5XF8.5) //)
          144 FORMAT (5X*K-ABSN EDGE JUMP RATIO*2XF8.4,7 (5XF8.4) //)
          145 FORMAT (35X*K-ALPHA PHOTONS NOT ABSORBED*//)
420      146 FORMAT (5X*KEP (J) *8 (5XF10.0) /)
          147 FORMAT (5X*K-FLUORESCENT YIELD*,8 (5XF8.5) //)
          149 FORMAT (5X*DENSITY*17XF8.4,7 (5XF8.4) //)
          150 FORMAT (5X*MASS ABSN COEF CONST K*2XF8.3,7 (5XF8.3) //)
          151 FORMAT (5X*MASS ABSN COEF CONST L*2XF8.3,7 (5XF8.3) //)
425      152 FORMAT (5X*MASS ABSN COEF EXPNT K*2XF8.3,7 (5XF8.3) //)
          153 FORMAT (5X*MASS ABSN COEF EXPNT L*2XF8.3,7 (5XF8.3) //)
          154 FORMAT (35X*K-ALPHA EMISSION DUE TO TERTIARY PHOTONS*//)
          155 FORMAT (5X*KTP (J) *8 (5XF10.0) //)
          170 FORMAT (I3, 8F10.5)
430      172 FORMAT (5X*KA1 (J) *8 (5XF10.0) //)
          173 FORMAT (//35X*PREDICTED RELATIVE INTENSITIES*10X*
          1BASED ON *I6* PHOTONS*//)
          174 FORMAT (5X*PRIMARY *3XF10.6,7 (5XF10.6) /)
          175 FORMAT (5X*SECONDARY*3XF10.6,7 (5XF10.6) /)
435      177 FORMAT (5X*TERTIARY *3XF10.6,7 (5XF10.6) /)
          178 FORMAT (//5X*TOTAL *3XF10.6,7 (5XF10.6) //)
          179 FORMAT (//35X*K-ALPHA EMISSION DUE TO PRIMARY PHOTONS*/)
          180 FORMAT (5X*ATOMIC WEIGHT *8 (5XF8.4) //)
          181 FORMAT (10F7.0)
440      182 FORMAT (7F10.6)
          183 FORMAT (2F5.3, F5.1, F7.3)
          210 FORMAT (//35X*RELATIVE INTENSITY = KA (J) /KA (J) 100*//)
          STOP
          END

```

APPENDIX B

X-RAYSA, A FORTRAN IV PROGRAM FOR NUMERICAL
REGRESSION ANALYSIS

PROGRAM XRAYSA

73/74

OPT=0 TRACE

FTN 4.6+428

```

1      PROGRAM XRAYSA (INPUT,OUTPUT,TAPE 5=INPUT,TAPE 6=OUTPUT)
C.....THIS PROGRAM USES MULTIPLE REGRESSION ANALYSIS TO
C.....OBTAIN X-RAYS FLUORESCENCE INFLUENCE COEFFICIENTS
C.....AND THEN USES THE GAUSS-JORDAN ELIMINATION METHOD
5      C.....TO OBTAIN THE CONCENTRATIONS (W/O), OF A SERIES OF
C.....OF ELEMENTS IN DIFFERENTS SAMPLES.
        DIMENSION C(20,20),A(20,20),ELEM(20),D(20,20),RM(20,20),
15      1SR(5),B(20),P(20),R(20),CI(20,20),CX(20,20),S(20),YM(20),
        2F(20,20),YY(20),DATA(20,20),STDI(20),RX(20),G(20,20)
10      READ (5,100) M,N,LS,KSW,CODE
        READ (5,101) (ELEM(J),J=1,M)
        NC=M+1
        IF (LS.EQ.1) GO TO 12
        XD=N-M
15      DO 3 I=1,N
3      READ (5,102) (RM(I,J),J=1,M)
        DO 4 I=1,N
4      READ (5,102) (C(I,J),J=1,M)
        DO 50 L=1,M
20      DO 2 K=1,N
        YM(K)=C(K,L)
        DO 2 I=1,M
        G(K,I)=C(K,I)*RM(K,L)
25      2 CONTINUE
C.....
        CALL MBA(G,N,M,20,YM,XD,0,SR,B,P,R,CI,CX,20,S)
C.....
        DO 6 I=1,M
30      6 A(L,I)=B(I)
50 CONTINUE
        WRITE (6,200) CODE
        WRITE (6,201) (ELEM(J),J=1,M)
        DO 7 I=1,M
35      7 WRITE (6,202) I,ELEM(I),(A(I,J),J=1,M)
        IF (KSW.EQ.2) STOP
        GO TO 15
C.....
C.....PROGRAM TO DETERMINE CONCENTRATIONS
C.....
40      12 READ (5,110) ((A(I,J),J=1,M),I=1,M)
15      READ (5,100) NS
        IF (LS.NE.1) WRITE (6,203) CODE
        IF (LS.EQ.1) WRITE (6,206) CODE
        WRITE (6,207)
45      WRITE (6,204) (ELEM(J),J=1,M)
        DO 20 KS=1,NS
        READ (5,102) (RX(I),I=1,M)
        DO 8 J=1,M
        DO 8 K=1,M
50      IF (K.EQ.J) F(K,K)=A(K,K)*RX(K)-1.
        IF (K.NE.J) F(J,K)=A(J,K)*RX(J)
        8 CONTINUE
        DO 14 J=1,NC
14      D(1,J)=1.
55      DO 16 J=2,NC
16      D(J,NC)=0.
        DO 13 J=1,M

```

PROGRAM XRAYSA

73/74

OPT=0 TRACE

FTN 4.6+428

```

      I=J+1
      DO 13 K=1,M
60      13 D(I,K)=F(J,K)
      C.....
      C.....START GAUSS-JORDAN ELIMINATION PROCESS
      C.....
      DO 11 K=1,M
65      KP1=K+1
      DO 9 J=KP1,NC
      9 D(K,J)=D(K,J)/D(K,K)
      D(K,K)=1.
      DO 11 I=1,M
70      IF (I.EQ.K.OR.D(I,K).EQ.0.) GO TO 11
      DO 10 J=KP1,NC
      10 D(I,J)=D(I,J)-D(I,K)*D(K,J)
      D(I,K)=0.
75      11 CONTINUE
      WRITE (6,205) K,(D(J,NC),J=1,M)
      20 CONTINUE
      C.....
      C.....END OF THE GAUSS-JORDAN PROCESS
      C.....
80      DO 40 J=1,NS
      40 READ (5,102) (DATA(J,K),K=1,M)
      WRITE (6,300)
      WRITE (6,204) (ELEM(J),J=1,M)
      DO 51 J=1,NS
85      51 WRITE (6,205) J,(DATA(J,K),K=1,M)
      C.....
      C.....INPUT AND OUTPUT FORMATS
      C.....
90      52 FORMAT (8F6.4)
      100 FORMAT (4I3,A3)
      101 FORMAT (8A2)
      102 FORMAT (8F6.4)
      110 FORMAT (8F10.8)
      200 FORMAT (1H1,35X*INFLUENCE COEFFICIENTS A(I,J) BASED
95      1ON *A3* DATA*//)
      201 FORMAT (5X*ELEMENT*11XA2,7(13XA2)/)
      202 FORMAT (5X,I2,1X,A2,4XF12.7,7(3XF12.7)/)
      203 FORMAT (///35X*CONCENTRATIONS BY X-RAYS FLUORESCENCE
100      1BASED ON *A3* DATA*//)
      204 FORMAT (5X*SAMPLE NUMBER*16XA2,7(11XA2),//)
      205 FORMAT (/9X,I3,13X,8(5XF8.6)/)
      206 FORMAT (1H1,35X*CONCENTRATIONS BY X-RAYS FLUORESCENCE
105      1ANALYSIS BASED ON*A3* DATA*//)
      207 FORMAT (36X*ELEMENT CONCENTRETION (W/O)*//)
      300 FORMAT (///35X*TRUE CONCENTRATIONS*//)
      STOP
      END

```

SUBROUTINE MRA

73/74 OPT=0 TRACE

PTN 4.6+428

```

1      SUBROUTINE MRA (X,M,N,MAXM,Y,D,K,SSR,B,P,R,AINV,C,MAXN,S)
C     MULTIPLE REGRESSION ANALYSIS
      DIMENSION X(1),Y(1),B(1),P(1),R(1),C(1),S(1),SSR(5)
      DIMENSION AINV(1)
5     C MATRIX OPCODES. 20=MULTIPLY, 23=TRANPOSE MULTIPLY,
C     10=INVERSE
C     Z=X TRANPOSE *Y, A INVERSE=(X TRANPOSE *X) INVERSE
      SQRTF(X) = SQRT(X)
      CALL MATRIX (23,M,N,1,X,MAXM,Y,M,P,N)
10     IF (K) 2,1,2
      1     CALL MATRIX (2,M,N,0,X,MAXM,AINV,0,0,0)
      CALL MATRIX (5,N,0,0,AINV,0,AINV,MAXN,0,0)
      CALL MATRIX (10,N,N,0,AINV,MAXN,B,0,0,0)
      IF(B(1)) 2,3,2
15     3     M=0
      GO TO 45
C     ESTIMATED COEFFICIENTS B=A INVERSE *Z, PREDICTED
C     VALUES P=X*B
      2     CALL MATRIX (20,N,N,1,AINV,MAXN,P,N,B,N)
      CALL MATRIX (20,M,N,1,X,MAXM,B,N,P,M)
20     C SSR(1) = SUM OF SQUARES OF RESIDUALS
      C SSR(2) = SUM OF SQUARES OF THE (Y(I)-MEAN)
      C SSR(3) = ESTIMATE OF ERROR VARIANCE
      C SSR(4) = SQUARED MULTIPLE CORRELATION COEFFICIENT
      C SSR(5) = MULTIPLE CORRELATION COEFFICIENT
25     C RESIDUALS R=Y-X*B
      SSR(1) = 0.0
      S(1) = 0.0
      DO 60 I=1,M
30         S(1) = S(1) + Y(I)
          R(I) = Y(I) - P(I)
      60     SSR(1) = SSR(1) + R(I) * R(I)
          S(1) = S(1) / M
          SSR(3) = SSR(1) / D
35     SSR(2) = 0.
      DO 70 I=1,M
          C(1) = Y(I) - S(1)
      70     SSR(2) = SSR(2) + C(1) * C(1)
          SSR(4) = (SSR(2) - SSR(1)) / SSR(2)
40     SSR(5) = SQRTF(SSR(4))
          JK= (N-1) * MAXN + 1
          DO 30 J=1,JK,MAXN
              JKK= J + N - 1
45     C VARIANCE-COVARIANCE MATRIX, C
          DO 30 I=J,JKK
      30     C(I) = AINV(I) * SSR(3)
C     ESTIMATES OF STANDARD ERRORS OF REGRESSION COEFFICIENTS
      DO 40 L=1,N
          I= (L-1) * MAXN + L
50     40     S(L) = SQRTF (C(I))
      45     RETURN
      END

```

LIST OF REFERENCES

- Adler, I., and Axelrod, J. M. (1955). Internal standards in fluorescent x-ray spectroscopy. *Spectrochim. Acta*, 7, 91.
- Alley, B. J., and Myers, R. H. (1965). Corrections for matrix effects in x-ray fluorescence using multiple regression methods. *Anal. Chem.*, 37, 1685.
- Andermann, G., and Allen, J. D. (1961). X-ray emission analysis of finishes cements. *Anal. Chem.*, 33, 1695.
- Andermann, G., and Kemp, J. W. (1958). Scattered x-ray as internal standards in x-ray emission spectroscopy. *Anal. Chem.*, 30, 1306.
- Archard, G. D., and Mulvey, T. (1963). The present state of quantitative x-ray microanalysis. Part 2: Computational methods. *Brit. J. Appl. Phys.*, 14, 626.
- Bambinek, W., Crasemann, B., Fink, R. W., Freund, H. V., Swift, C. D., Price, R. E., and Rao, P. V. (1972). X-ray fluorescence yields, Auger, and Coster-Kronig transition probabilities. *Rev. Mod. Phys.*, 44, 716-813.
- Beattie, H. J., and Brissey, R. M. (1954). Calibration method for x-ray fluorescence spectrometry. *Anal. Chem.*, 26, 980.
- Bertin, E. P. (1964). Intensity ratio technique for x-ray spectrometric analysis of binary samples. *Anal. Chem.*, 36, 826.
- _____. (1970). Principles and Applications of X-Ray Spectrometric Analysis. New York: Plenum Press.
- Birks, L. S. (1959). X-Ray Spectrochemical Analysis. New York: Interscience.
- Birks, L. S., Ellis, D. J., and Grant, B. K. (1966). The Electron Microprobe. New York: John Wiley and Sons.
- Bishop, H. E. (1965). A Monte Carlo calculation on the scattering of electrons in copper. *Proc. Phys. Soc.*, 85, 855.
- Blavier, P., Hans, H., Tyou, P., and Houbart, I. (1960). Elemental analysis of alnico type alloys by x-ray fluorescence. *Cobalt*, 7, 33.

- Bruch, J. (1962). Application of x-ray fluorescence analysis to study of various ferro alloys. *Archiv. Eisenhüttenwesen*, 33, 5.
- Burham, H. D., Howser, J., and Jones, L. C. (1957). Generalized x-ray emission spectrographic calibration applicable to varying composition and sample forms. *Anal. Chem.*, 29, 1827.
- Campbell, W. J., and Carl, H. F. (1954). Quantitative analysis of niobium and tantalum in ores by fluorescent x-ray spectroscopy. *Anal. Chem.*, 26, 800.
- _____. (1956). Fluorescent x-ray spectrographic determination of tantalum in commercial niobium oxides. *Anal. Chem.*, 28, 960.
- Campbell, W. J., and Thatcher, J. W. (1962). Fluorescent x-ray spectrography -- Determination of trace elements. U. S. Bur. Mines Rep. Invest. 5966.
- Claisse, F. (1957). Accurate x-ray fluorescence analysis without internal standard. *Norelco Rep.*, 4, 3.
- Claisse, F., and Quintin, M. (1967). A mathematical analysis of the inter-element effects in x-ray fluorescence. *Can. Spectrosc.*, 12, 129.
- Colby, J. W. (1968). Quantitative microprobe analysis of thin insulating films. *Advan. X-Ray Anal.*, 11, 287.
- Compton, A. H., and Allison, S. K. (1935). X-Ray in Theory and Experiment. New York: D. Van Nostrand Co.
- Criss, J. W., and Birks, L. S. (1968). Calculation methods for fluorescent x-ray spectrometry. *Anal. Chem.*, 40, 1080.
- Cullen, T. J. (1962). Coherent scattered radiation internal standardization in x-ray spectrometric analysis of solutions. *Anal. Chem.*, 36, 1098.
- Davis, E. N., and Van Nordstrand, R. A. (1954). Determination of barium, calcium and zinc in lubricating oils. *Anal. Chem.*, 26, 937.
- Fagel, J. E., Jr., Liebhafsky, H. A., and Zeman, P. D. (1958). Determination of tungsten or molybdenum in x-ray emission spectroscopy. *Anal. Chem.*, 30, 1918.
- Gardner, R. P., and Hawthorne, A. R. (1975). Monte Carlo simulation of the x-ray fluorescence excited by discrete energy photons in homogeneous samples including tertiary inter-element effects. *X-Ray Spectrom.*, 4, 138-148.

- Gilfrich, J. V., and Birks, L. S. (1968). Spectral distribution of x-ray tubes for quantitative x-ray fluorescence analysis. *Anal. Chem.*, 40, 1077.
- Gillman, E., and Heal, H. T. (1952). Some problems in the analysis of steel by x-ray fluorescence. *Brit. J. Appl. Phys.*, 3, 353.
- Glocker, R., and Schreiber, H. (1928). Quantitative roentgen spectrum analysis by means of cold excitation of the spectrum. *Ann. Phys.*, 85, 1089-1102.
- Green, M. (1963). A Monte Carlo calculation of the spatial distribution of characteristic x-ray production in a solid target. *Proc. Phys. Soc.*, 82, 204.
- Guinier, A. (1961). X-ray fluorescence analysis -- uses and limitations. *Rev. Univers. Mines*, 17, 143.
- Gunn, E. L. (1957). Fluorescent x-ray spectral analysis of powdered solids by matrix dilution. *Anal. Chem.*, 29, 184.
- _____. (1961). X-ray fluorescence intensity of elements evaporated from solution onto thin films. *Anal. Chem.*, 33, 921.
- Hamos, V. L. (1945). On the determination of very small quantities of substances by the x-rays microanalysis. *Arkiv. Math. Astrom. Fysics.*, 31A, 1.
- Hakkila, E. A., and Waterbury, F. (1960). X-ray fluorescence spectrographic determination of impurities and alloying elements in tantalum container materials. *Talantla*, 6, 46.
- Heinrich, K. F. J. (1966). X-ray absorption uncertainty. In The Electron Microprobe, T. D. McKinley, K. F. J. Heinrich, and D. B. Witry (eds.). New York: John Wiley and Sons.
- Hevesy, G., and Alexander, E. (1933). X-ray fluorescence in chemical analysis. *Akad. Verlagsges, Leipzig*.
- Hirokawa, K. (1962). Determination of alloyed elements in special steels by x-ray fluorescent x-rays. I. Nickel and chromium in nickel-chromium steel and tungsten in tungsten steel. *Sci. Rep. Inst. Tohoku Univ. Ser. A*, 14, 278.
- International Tables for X-Ray Crystallography (1962). Birmingham, England: Kynoch Press.
- Jenkins, R., and de Vries, J. L. (1967). Practical X-Ray Spectrometry, Phillips Technical Library. New York: Springer-Verlag.
- Jones, R. A. (1961). Determination of sulfur in gasoline by x-ray emission spectrography. *Anal. Chem.*, 33, 71.

- Kemp, J. W., Hasler, M. F., and Jones, J. L. (1954). Outline of fluorescent x-ray spectroscopy. A. R. L. Spectrographer's Newsletter, 7, 3.
- Koh, P. K., and Caugherty, B. (1952). Metallurgical applications of x-ray fluorescent analysis. J. Appl. Phys., 23, 427.
- Kramers, H. A. (1923). Theory of x-ray absorption and of the continuous x-ray spectrum. Phil. Mag., 46, 836.
- Lachance, G. R., and Traill, R. J. (1966). A practical solution to the matrix problem in x-ray analysis. Can. Spectrosc., 11, 43.
- Lambert, M. C. (1959). Some practical aspects of x-ray spectrography. Norelco Rep., 6, 31.
- Leraux, J. (1962). Method for finding mass-absorption coefficients by empirical equations and graphs. Advan. X-Ray Anal., 5, 153.
- Lincoln, A. J., and Davis, E. N. (1959). Determination of platinum in alumina base reforming catalyst by x-ray spectroscopy. Anal. Chem., 31, 1317.
- Lucas-Tooth, H. J., and Price, B. J. (1961). A mathematical method for the investigation of interelement effects in x-ray fluorescent analyses. Metallurgia, 64, 149.
- Mitchell, B. J., and O'Hear, H. J. (1966). General x-ray spectrographic solution method for iron, chromium, and/or manganese-bearing materials. Anal. Chem., 34, 1620.
- Muller, R. O. (1972). Spectrochemical Analysis by X-Ray Fluorescence, translated by K. Keil. New York: Plenum Press.
- Noakes, G. E. (1954). An absolute method of x-ray fluorescence analysis applied to stainless steels. ASTM Spec. Tech. Publ., 157, 57.
- Pluncherry, M. (1963). Absolute method for x-ray fluorescence analysis applicable to films obtained by vacuum evaporation of iron-nickel alloys. Spectrochim. Acta, 19, 533.
- Preis, H., and Esenwin, A. (1959). X-ray fluorescence spectrographic method for determination of lead in gasoline. Schweizer Archiv., 26, 317.
- Rasberry, S. D., and Heinrich, K. F. J. (1974). Calibration for interelement effects in x-ray fluorescence analysis. Anal. Chem., 46, 81.

- Renaud, M. (1963). Derivation of the matrix effects in x-ray fluorescence. *Comptes rendus*, 256, 3086.
- Reynolds, R. C. (1963). Matrix corrections in trace element analysis by x-ray fluorescence -- Estimation of mass absorption coefficients by Compton scattering. *Amer. Mineral.*, 48, 1133.
- Rhodin, T. N. (1955). Chemical analysis of thin films by x-ray emission spectrography. *Anal. Chem.*, 27, 1857.
- Rose, H. J. (1960). X-ray fluorescence spectroscopy in the analysis of ores, minerals, and waters. *Advan. X-Ray Anal.*, 11, 23.
- Ryland, A. L. (1964). A general approach to the x-ray spectroscopic analysis of samples of low atomic number. *Nat. Meet. Am. Chem. Soc.*, 14th, Philadelphia.
- Sherman, J. (1954). The correlation between fluorescent x-ray intensity and chemical composition. *ASTM Spec. Tech. Publ.*, 157, 27.
- _____. (1955). The theoretical derivation of fluorescent x-ray intensities from mixtures. *Spectrochim. Acta*, 7, 283.
- Shiraiwa, T., and Fujino, N. (1966). Theoretical calculation of fluorescent x-ray intensities in fluorescent x-ray spectrochemical analysis. *Japan J. Appl. Phys.*, 5, 886.
- Wagner, J. C., and Bryan, F. R. (1966). X-ray spectrographic analysis of automotive combustion deposits without the use of calibration curves. *Advan. X-Ray Anal.*, 9, 528.
- Wang, M. S. (1962). Rapid sample fusion with lithium tetra borate for emission spectroscopy. *Appl. Spectroscopy*, 16, 141.